REPOSITORY PNL
COLLECTION Atmospheric Releases
BOX No. N/A
FOLDER N/A

727756

BNWL-SA-1435

R

ON THE VARIANCE OF CONCENTRATION[1] IN PLUMES AND WAKES

by

Warren Ted Hinds

Environmental and Radiological
Sciences Department

BATTELLE MEMORIAL INSTITUTE
Pacific Northwest Laboratory

Richland, Washington

September, 1967

(1) Work performed under Contract No. AT(45-1)-1830 between the Atomic Energy Commission and Battelle-Northwest.

1204906

TABLE OF CONTENTS

		Page
INTRODUCTION		vi
ACKNOWLEDGMENTS		vii
CHAPTER ONE -	THEORETICAL BACKGROUND	1
	Concentration Fluctuations	1
	The Governing Equation	3
	Approximate Solutions to the Governing Equation	9
	Wake Structure and Diffusive Character	11
CHAPTER TWO -	EXPERIMENTAL METHODS	16
	Tracer Technique	16
	Sampling Techniques	17
	Design of the Sampling Grids	22
	Field Procedures	24
CHAPTER THREE -	DATA REDUCTION AND PRESENTATION	26
	Mean Concentration Patterns	27
	Time History of Concentration	28
CHAPTER FOUR -	DATA ANALYSIS	32
	Distribution of Observed Concentrations	32
	Variance of Concentration	33
	Peak-to-Mean Concentration Ratios	41
SUMMARY AND CONCLUSIONS		51
REFERENCES		53
APPENDIX - FIVE-SECOND AVERAGES OF CONCENTRATION		57

1204907

LIST OF FIGURES

Figure		Page
1	Shift of Record when $f(\tau)$ is Changed to $f(\tau \pm t/2)$	6
2	Schematic Planview of Wake Structure	12
3	Tracer Dispenser and Associated Equipment	18
4	The Self-Orienting Sampler	19
5	The Self-Orienting Real Time Sampler	21
6	The Control Sampling Grid	23
7	The Wake Sampling Grid	25
8	Mean Concentration Isopleths for Control Test C-3	28
9	Mean Concentration Isopleths for Control Test C-4	29
10	Mean Concentration Isopleths for Wake Test W-6	30
11	Mean Concentration Isopleths for Wake Test W-7	31
12	Frequency Distributions of Concentration Ratio $\chi/\bar{\chi}$	34
13	Composite Frequency Distribution of Concentration Ratio $\chi/\bar{\chi}$	35
14	Fractional Decrease in Variance With Increasing Smoothing Interval, Control Test C-3	37
15	Fractional Decrease in Variance With Increasing Smoothing Interval, Control Test C-4	38
16	Fractional Decrease in Variance With Increasing Smoothing Interval, Wake Test W-6	39
17	Fractional Decrease in Variance With Increasing Smoothing Interval, Wake Test W-7	40
18	Calculated and Observed Autocovariance Function, Control Test C-3	42

1204908

Figure Page

19 Calculated and Observed Autocovariance Function, Control Test C-4 43

20 Calculated and Observed Autocovariance Function, Wake Test W-6 44

21 Calculated and Observed Autocovariance Function, Wake Test W-7 45

22 Fractional Decrease in Variance vs Smoothing Interval With Exponential Form of $P(t/2)/\sigma_s^2$ 46

23 Peak-to-Mean Concentrations vs Proportional Sampling Time . 48

24 Peak-to-Mean Concentrations vs Sampling Interval 49

1204909

LIST OF TABLES

Table		Page
I	Mean, Variance and Standard Deviation from Four Tests, Measured by the SORTS	33
II	Constants b and k for Four Tests	41

1204910

INTRODUCTION

In recent years, a great deal has been learned concerning diffusion in the atmosphere. Attention has occasionally been turned to variations in concentration level with time and space, as well as to the more familiar study of patterns of average concentrations; the term "peak-to-mean" or "peak-to-average" concentration ratio has become an increasingly more frequent item for discussion in the literature. The resulting search for methods to rationalize observed peak-to-mean concentration ratios led to hypotheses concerning the relation of the variance of concentration to the averaging interval applied to the concentration before the variance is calculated. It is my purpose here to show how an explicit formulation of this relationship can be derived, and to check the results of the theoretical work with observed concentration behavior.

The experimental designs chosen to provide concentration data provided a substantial contrast in turbulent characteristics, since the theory developed here is independent of turbulence. One set of data was gathered in a plume from a point source, another in the lee of a building with the source near the upwind stagnation point, thus yielding data from both atmospheric and "aerodynamic" turbulence.

In the following pages, the derivation of the governing equation and a brief description of the character of wake flow is given. (A complete discussion of point source plumes can be found in Pasquill, 1962.) The experimental techniques employed are described, the data obtained are given, and a comparison of the data with the theoretical formulation is carried out.

1204911

ACKNOWLEDGMENTS

Professor K. J. K. Buettner, Chairman of my thesis committee, offered a helping hand in this work in all phases. I am keenly aware of and grateful for his early expressions of confidence, without which my task would have seemed difficult indeed.

My thanks also go to Professor J. A. Businger, for his even-handed appraisal of steps along the way, and Dr. C. E. Elderkin of the Pacific Northwest Laboratory, for many suggestions and discussions of alternatives.

Finally, my sincere thanks to B. N. Nelson, Jr.; his deceptively simple design of the SOS and SORTS air samplers made the awkward task of sampling in wakes a straightforward procedure.

1204912

CHAPTER ONE

THEORETICAL BACKGROUND

In this chapter, the derivation of an equation relating the variance of an increasingly smoothed variable to the smoothing interval is given, and the character of wake flow is discussed.

Concentration Fluctuations

Fundamentally, the cause of concentration variation is turbulent motion which wafts the plume of contaminant or tracer over and away from the sampler. This separation into instantaneous and mean plumes is a familiar tack in meteorology; much more is known experimentally about the latter than the former, so relation of variation in concentration is usually made to the mean concentration.

Two rather different approaches to rationalizing the variation of concentration have been suggested. Gifford (1959) considered a plume to consist of an infinite series of diffusing disks, each with a gaussian distribution within itself, which through atmospheric meander combine to produce a gaussian distribution of concentration at points within the mean plume. One deduction from this model was that the peak concentration observed at a point, normalized to the mean concentration at that point, must decrease as a power law of distance from the source if the point were near the centerline, and nearly as a power law in any case.

A different starting point led Csanady (1967) to rather different expressions for the variation of concentration at a point in a plume. Starting with the equation of continuity, he derived a conservation statement for variance of concentration, then deduced a formulation for the variance as a function of distance from the centerline of a slender

1204913

plume. Presuming the distribution of concentration observed at a point throughout time to be akin to a Poisson distribution, he showed approximately the magnitude of peak-to-mean concentrations to be expected as a function of distance from source point and centerline of the plume.

It should be noted that two types of peak concentration can be defined. One, as discussed by Gifford and Csanady, considers variability of concentration in relation to plume centerline. Another results from averaging the time history of concentration at a point over differing intervals, that is, considering the concentration to be a random function of time, the observed peak concentration will be a decreasing function of smoothing interval. Gifford (1960) presents a number of data from several workers which indicates the effect of increasingly smoothing concentration measurements. A fairly well defined power law dependence results, with the index a function of displacement from the plume centerline. Singer (1960) presents a summarization of data which indicates a power law dependence, also. In a later paper, Singer et al. (1963) present a nearly independent set of data, again from a number of workers, which also indicates a power law dependence of peak-to-mean ratio on smoothing interval. Recognizing that the peak concentration can be specified in terms of standard deviation of the distribution of concentration observed through time (see Csanady, 1967), Singer and his co-workers (1963) hypothesized that a power law connected variance and smoothing interval.

Not all data indicate a strict power law, however, Faoro (1965) presents data which indicate that the index may be a function of smoothing interval, and Genikhovich and Gracheva (1965) in an examination of

1204914

horizontal dispersion derived a sum of exponential, inverse-linear, and inverse-square terms for the decrease of variance with smoothing interval.

The Governing Equation

The effect of smoothing a variable before calculating the variance is presented in a formal representation of filtering and its effect on Fourier components in Pasquill (1962), but no explicit relationship is developed. An expression for the change in variance with change in smoothing interval follows from a consideration of the definition of the variance of a smoothed function.

Let X be a singled valued, continuous stationary random variable

τ be time, the independent variable

t be the (relatively) short smoothing interval

T be the (relatively) long length of record

X_s be the smoothed value of X, over the interval t

$\overline{X}$ be the average value of X, over the interval T

σ_s^2 be the variance of X_s over the interval T

The smoothed variable is defined by

$$X_s = \frac{1}{t}\int_{\tau-t/2}^{\tau+t/2} X(\lambda)\, d\lambda \qquad (1)$$

where a dummy variable λ has been introduced as the variable of integration. The definition of variance in terms of X_s is then

$$\sigma_s^2 = \frac{1}{T}\int_{-T/2}^{T/2} (X_s - \overline{X})^2\, d\lambda \qquad (2)$$

1204915

It may be noted that the operation of smoothing X over periods of length t yields a continuous variable if overlapping means are considered, and a discrete variable if end-to-end means are considered. Here overlapping means will be assumed.

Expanding $(X_s - \overline{X})^2$ and differentiating with respect to t yields

$$\frac{d\sigma_s^2}{dt} = \frac{1}{T} \int_{-T/2}^{T/2} \left(2X_s \frac{dX_s}{dt} - 2\overline{X} \frac{dX_s}{dt}\right) d\lambda \tag{3}$$

The derivative of X_s is a function of the limits on the integral (1) (when the integral is differentiated) and X_s,

$$\frac{dX_s}{dt} = -\frac{1}{t} X_s + \frac{1}{t}\left[X(\tau+t/2) \frac{d(\tau+t/2)}{dt} - X(\tau-t/2) \frac{d(\tau-t/2)}{dt}\right]$$

$$= -\frac{1}{t} X_s + \frac{1}{t}\left[\frac{1}{2} X(\tau+t/2) + \frac{1}{2} X(\tau-t/2)\right]$$

For simplicity, let $\frac{1}{2}\left[X(\tau+t/2) + X(\tau-t/2)\right]$ be defined as X_L.

Then

$$\frac{dX_s}{dt} = \frac{1}{t}(X_L - X_s) \tag{4}$$

Inserting this expression for dX_s/dt in Equation 3 yields

$$\frac{d\sigma_s^2}{dt} = \frac{2}{t}\left[\underset{\text{(I)}}{\frac{1}{T}\int_{-T/2}^{T/2} X_s X_L d\lambda} - \underset{\text{(II)}}{\frac{1}{t}\int_{-T/2}^{T/2} X_s^2 \, d\lambda} - \underset{\text{(III)}}{\frac{1}{T}\int_{-T/2}^{T/2} \overline{X} X_L d\lambda} + \underset{\text{(IV)}}{\frac{1}{T}\int_{-T/2}^{T/2} \overline{X} X_s d\lambda}\right] \tag{5}$$

Each of the numbered integrals will now be examined.

1204916

First, consider Integral IV in Equation 5. It can be written as

$$\bar{X}\left[\frac{1}{T}\int_{-T/2}^{T/2} X_s\,d\lambda\right] \tag{6}$$

This is just the average of X_s over the interval -T/2 to T/2, which is equal to $\bar{X}$. Thus

$$\frac{1}{T}\int_{-T/2}^{T/2} \bar{X}X_s\,d\lambda = \bar{X}^2 \tag{7}$$

Consider now Integral III. This can be written

$$\frac{1}{T}\int_{-T/2}^{T/2} \bar{X}X_L\,d\lambda = \frac{\bar{X}}{2T}\int_{-T/2}^{T/2} X(\lambda+t/2)\,d\lambda + \frac{\bar{X}}{2T}\int_{-T/2}^{T/2} X(\lambda-t/2)\,d\lambda \tag{8}$$

These are integrals of X over a slightly different record than originally used to define $\bar{X}$ and σ_s^2, with a shift in record of t/2 at each end of the interval -T/2 to T/2, as shown in Figure 1. The first integral in Equation 8 involves a loss of t/2 length at -T/2, and a gain of t/2 length beyond T/2. Conversely, the second integral involves a gain of t/2 length at -T/2 (i.e., integration over a portion of X preceding -T/2) and a loss of t/2 length of the original record at T/2. Thus, the first integral in Equation 8 is (ignoring $\bar{X}$ for the moment)

$$\frac{1}{2}\left[\frac{1}{T}\int_{-T/2}^{T/2} X(\lambda+t/2)\,d\lambda\right] = \frac{1}{2}\left[\frac{1}{T}\int_{-T/2}^{T/2} X(\lambda)\,d\lambda - \frac{1}{T}\int_{-T/2}^{-T/2+t/2} X(\lambda)\,d\lambda + \frac{1}{T}\int_{T/2}^{T/2+t/2} X(\lambda)\,d\lambda\right] \tag{9}$$

1204917

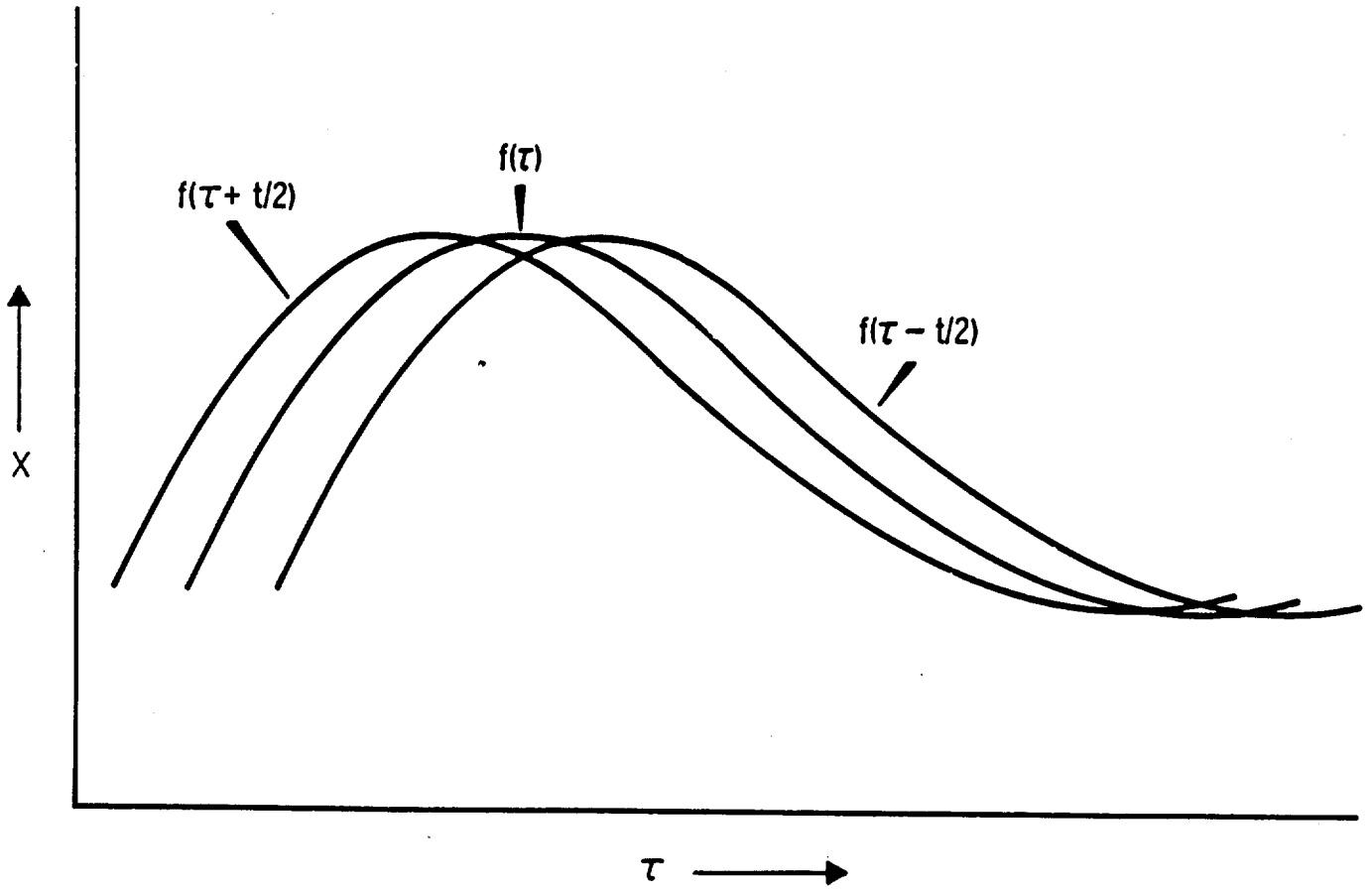

Figure 1
Shift of Record when $f(\tau)$ is Changed to $f(\tau \pm t/2)$

1204918

while the second integral is

$$\frac{1}{2}\left[\frac{1}{T}\int_{-T/2}^{T/2} X(\lambda - t/2)d\lambda\right] = \frac{1}{2}\left[\frac{1}{T}\int_{-T/2}^{T/2} X(\lambda)d\lambda + \frac{1}{T}\int_{-T/2-t/2}^{-T/2} X(\lambda)d\lambda - \frac{1}{T}\int_{T/2-t/2}^{T/2} X(\lambda)d\lambda\right] \tag{10}$$

After summing Equations 9 and 10, it can be seen that the Integral III in Equation 5 is very nearly $\overline{X^2}$. The difference between Integral III and $\overline{X^2}$ is only that due to interchange of -t/2 -T/2 with -T/2 +t/2 and T/2 -t/2 with T/2 +t/2, that is the record within t/2 outside the bounds of the original record is added and the record within t/2 inside the bounds of the original record is deleted. This odd manipulation results from the differentiation of the limits on X_s. Nevertheless, if X is stationary, an assumption implicit in this entire argument, the sum of Equation 9 and 10 is very nearly $\overline{X^2}$.

Now, both Integral III and IV in Equation 5 have been shown to be (very nearly) $\overline{X^2}$, but with opposite sign.

Consider now Integral I in Equation 5. The integrand can be written as a product of mean and fluctuating values:

$$X_s X_L = (\overline{X}_s + X_s')\ (\overline{X}_L + X_L') = (\overline{X} + X_s')\ (\overline{X} + X_L')$$

$$= \overline{X}^2 + \overline{X}X_L' + \overline{X}X_s' + X_s'X_L'$$

since $\overline{X}_s = \overline{X}_L = \overline{X}$ as shown above. When each term is averaged over the interval -T/2 to T/2,

$$\overline{X_s X_L} = \overline{X}^2 + \overline{X_s' X_L'} \tag{11}$$

1204919

A similar procedure applied to Integral II in Equation 5 yields

$$\overline{X_s^2} = \overline{(\overline{X} + X_s')^2} = \overline{X}^2 + 2\overline{XX_s'} + \overline{X_s'^2} = \overline{X}^2 + \overline{X_s'^2} \tag{12}$$

Thus Equation 5 can be written as

$$\frac{d\sigma_s^2}{dt} = \frac{2}{t}\left[\overline{X}^2 + \overline{X_s'X_L'} - \overline{X}^2 - \sigma_s^2\right] = \frac{2}{t}\left[\overline{X_s'X_L'} - \sigma_s^2\right] \tag{13}$$

An insight into the character of $X_s'X_L'$ is possible by defining $X_s'(\tau)$ in terms of $X'(\tau)$, the primitive deviation of the function from the mean. At any time τ (the midpoint of the interval over which X_s is defined) we may write

$$X'(\tau) = X_s'(\tau) + X_s''(\tau) \tag{14}$$

Then, using the expanded form of X_L,

$$\overline{X_s'X_L'} = \overline{\left[X'(\tau) + X''(\tau)\right]\left[\frac{1}{2}X'(\tau+t/2) + \frac{1}{2}X'(\tau-t/2)\right]}$$

or, if $X(\tau)$ is stationary, so that $\overline{X'(\tau)\ X'(\tau+t/2)} = \overline{X'(\tau)\ X'(\tau-t/2)}$,

$$\overline{X_s'X_L'} = \overline{X'(\tau)\ X'(\tau+t/2)} + \overline{X_s''(\tau)\ X'(\tau+t/2)} \tag{15}$$

Equation 15 indicates that $\overline{X_s'X_L'}$ is closely related to the autocovariance of X at lag t/2. The term $\overline{X_s''(\tau)\ X'(\tau+t/2)}$ approaches zero by definition as $t \to 0$, and must finally approach zero at large t, since it is a correlation. A maximum value may be attained at some lag time, but the magnitude cannot be large and seems likely to be zero, since 1) X_s' is itself small compared to X', and 2) X_s'' may be either positive or negative for a given sign on X'. Thus, to a good approximation,

$$\overline{X_s'X_L'} = \overline{X'(\tau)\ X'(\tau+t/2)} \tag{16}$$

1204920

Let $P(t/2) = \overline{X'(\tau)\ X'(\tau+t/2)}$, so that Equation 13 may be written

$$\frac{d\sigma_s^2}{dt} + \frac{2}{t}\sigma_s^2 = \frac{2}{t}P(t/2) \tag{17}$$

or

$$\frac{d\sigma_s^2}{\sigma_s^2} = 2\left[\frac{P(t/2)}{\sigma_s^2} - 1\right]\frac{dt}{t} \tag{18}$$

Equation 17 or 18 is the expression of the dependence of variance on smoothing interval which was sought.

Approximate Solutions of the Governing Equation

The existence of an explicit and unique solution to Equation 17 or 18 is dependent upon the existence of an explicit function for $P(t/2)$, a very restrictive condition in a practical sense. However, good results may be expected by assuming merely plausible forms for $P(t/2)$, since much of the error introduced by an erroneous form for $P(t/2)$ will be smoothed out by the integration; any reasonably accurate form for $P(t/2)$ will serve the purpose.

Note that $P(t/2)/\sigma_s^2$ is approximately an autocorrelation of X at lag $t/2$. However, the normalizing variance is σ_s^2 rather than the total variance, so $P(t/2)/\sigma_s^2$ must decrease less rapidly and regularly than the autocorrelation $R(t/2)$. Nevertheless, if $P(t/2)/\sigma_s^2$ is interpreted as an autocorrelation of the form e^{kt} in Equation 18, the solution is

$$\frac{\sigma_s^2}{\sigma_{s,o}^2} = 2\sum_{n=1}^{\infty}\frac{k^n(t^n - t_o^n)}{n\ n!} \tag{19}$$

Since k is negative, this is an alternating series which, although convergent for all t, converges slowly at even moderate values of $t > 1$.

1204921

One of the simplest approximations which may be made for the solution of Equation 18 is to presume that

$$\frac{d\sigma_s^2}{\sigma_s^2} = (b+kt)\,\frac{dt}{t} \tag{20}$$

from which, by comparing Equation 18 and 20,

$$P'(t/2) = \frac{1}{2}\,(2+b+kt)\,\sigma_s^2. \tag{21}$$

Thus, an estimate, $P'(t/2)$, of the autocovariance function, $P(t/2)$, is possible by direct calculation, if b and k are known. If Equation 21 accurately reflects autocovariance data, then the linear approximation made in Equation 20 is probably adequate. It is clear that any benefits from integrating an approximate form are lost in the calculation of $P'(t/2)$. Nevertheless, it will be shown later that Equation 21 yields rather good estimates of the autocovariance function.

The constants b and k can be evaluated from a comparison of the solution to Equation 20 with data. The solution is

$$\frac{\sigma_s^2}{\sigma_{s,o}^2} = \left(\frac{t}{t_o}\right)^b e^{k(t-t_o)} \tag{22}$$

so that b can be calculated from a point at small values of t/t_o, and k at a large value to t/t_o. Another check of the theory then results from a complete comparison of Equation 22 with $\sigma_s^2/\sigma_{s,o}^2$ data at all intermediate t/t_o.

Note that if Equation 20 is simplified to

$$\frac{d\sigma_s^2}{\sigma_s^2} = b\,\frac{dt}{t} \tag{23}$$

1204922

an equation identical to that hypothesized by Singer et al. (1963) results.

Wake Structure and Diffusive Character

There are several descriptions of the formation and structure of wakes available in the literature (Birkhoff et al., 1957; Halitsky, 1963; Martin, 1965) so only a brief definition of terms is required here. Figure 2 indicates the several portions of the wake as described by Halitsky. Of most importance in the present discussion is the displacement zone and the cavity. The displacement zone is the volume of air near the building which is characterized by streamlines curved around the obstruction. The inner portion of the displacement zone is marked by a rather stationary series of vortices generated by severe flow distortion at the building edges and corners. The vortices are dependent upon the upstream speed and direction; changes in direction, especially, cause the vortices to be shed from their sites and carried downwind, to be replaced by a new geometry of vortex placement depending upon the new wind condition. The vortices provide a mechanism by which material originally outside the wake streamlines becomes enmeshed in the cavity, the stationary eddy attached to the downwind side of the building. The cavity is marked by a weak upwind flow, a decrease in wind speed and increase in turbulent intensity.

Separation of flow to cause the cavity and wake depends strongly upon the geometry of the obstacle; in general, circular shapes show a variable point of separation, depending upon wind speed, while prismoidal shapes characteristically induce separation at the upwind or lateral corners. The line of separation is important in delineating the

1204923

SCHEMATIC OF WAKE STRUCTURE

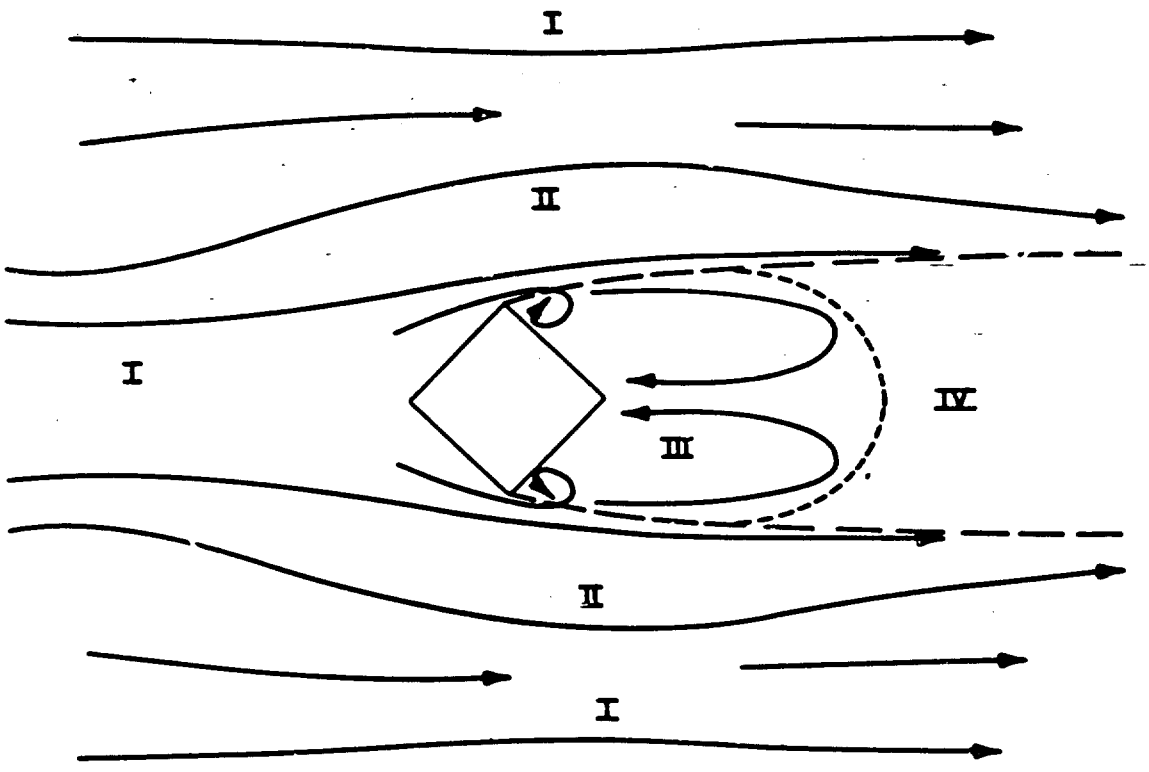

I Free Stream Flow

II Displacement Zone

III Cavity

IV Wake

Figure 2
Schematic Planview of Wake Structure

1204924

volume of contaminated air if the pollutant is released directly into the cavity, since little contamination of the obstacle upstream of the separation is possible. (This is clearly inapplicable to pollutant introduced upwind of the separation point.)

The shape of the wake is approximately independent of the obstacle shape, being paraboloidal downstream of the obstacle (Birkhoff, 1957). However, the shape of the cavity is closely related to the obstacle shape, since the upstream boundary of the cavity is the obstacle itself. Evans (1957) showed a variety of cavity shapes due to a variety of obstacle shapes; in general, the cavity shape varied more slowly with modulation of obstacle shape than did the obstacle itself.

The placement of the source is an important parameter in determining the final pattern of contamination. Halitsky (1963a, 1963b) shows this explicitly in a series of illustrations. It is illuminating to note that his data indicate that very short stacks, say less than one-half obstacle diameter in height, are little if any different from flush vents (Halitsky, 1963a, 1965) for introducing contaminants into the wake. His work shows that nearly all positions of source point with respect to the prevailing wind produce similar patterns of contamination in the cavity. The exception is a source placed at the outer edge of the obstruction, in which case a strongly assymetrical pattern in the cavity results; still, a substantial degree of contamination throughout the cavity is evidenced, apparently due to the mixing induced by vortices detached from the building separation line.

Entrainment of emissions from short stacks has captured the greater interest of workers to date, particularly in field studies. Since

1204925

emission from short stacks is only intermittently entrained in the cavity or wake (c.f. Sherlock and Stalker, 1940; Hohenleiten and Wolf, 1952), this is inherently a more complicated study than considering ground level or flush-vent sources. Nevertheless, nearly all information available concerning diffusion in wakes is from stacks. Davies and Moore (1964) used wind and water tunnels to model the flow about a reactor building, then carried out a verification of the tunnel studies in the field. They succeeded in modeling the behavior of effluent and wind speed interaction showing that a critical effluent-to-wind speed ratio governed the entrainment of the plume. Munn and Cole (1965), using a portable sampling system and bivane measurement of horizontal and vertical turbulent intensity, tested a variety of diffusion models used for estimating concentrations in building wakes (Barry, 1964), and verified at least qualitatively Davies and Moore's claim.

Martin (1965) carried out an ambitious and informative comparison of wind tunnel and full scale diffusion experiments, verifying the usefulness of wind tunnel work for estimating diffusive capacities of the atmosphere. Martin's work demonstrated both qualitative and quantitative correspondence of wind, wake and obstacle, thus enhancing the value of thorough wind tunnel tests.

Islitzer (1965) measured the effects of buildings on both turbulence and diffusion using a ground source in the lee of a reactor complex. He found that in unstable conditions the effect of the wake is essentially damped out in 800 meters of travel, and that the effect of an obstacle is to reduce the wind speed (outside the cavity) by some 30%, and increase the turbulent intensity. Thus, he found a net decrease in concentration

1204926

in the lee of the building relative to unobstructed sources. Culkowski (1967) later suggested that point source ground release results provide an absolute upper bound on mean concentrations in wakes.

1204927

CHAPTER TWO

EXPERIMENTAL METHODS

The general method for measuring the diffusive character of the atmosphere is to release an inert tracer in a specified fashion and measure the resulting concentration (or related parameter) at one or several points downwind. The techniques used in the present series were evolved from the rather well-known methods previously used in larger scale experiments carried out at Hanford and other sites. In this chapter, the tracer and the method of its dispersal are described, the sampling techniques and instruments are discussed, and the layout of the sampling geometry is shown.

Tracer Technique

The atmospheric tracer material used during these experiments was the fluorescent pigment zinc sulfide, U. S. Radium Corporation designation No. 2210. It is a very fine particulate that fluoresces green under ultraviolet light. The particle size distribution is nearly log normal with a geometric mean of about 2.5 microns and a standard deviation of logarithms of the diameter of 0.70. The density of the zinc sulfide particles is 4.1 grams per cc.

Ordinarily, the tracer is suspended in water for dispersal through high volume insecticidal foggers. In the present case, the use of water as the suspension agent was thought to be impractical, since some travel distances on the order of only a few meters were used, which might well preclude complete evaporation of the droplets. A dry cleaning solvent, trichloroethane, was substituted; this liquid has a very high vapor pressure at normal temperatures, and evaporates completely within a

1204928

meter. A small backpack type of herbicide dispenser (manufactured by Solo Kleinmotoren), which used a high speed air flow to break up the tracer suspension into small droplets, proved to be a satisfactory low flow dispenser. Figure 3 shows the sprayer and associated equipment.

Sampling Techniques

Two types of air sampling were conducted during this series of tests: time-integrated concentrations, and time history of concentration. The time-integrated concentrations were comparable to the standard measurements as made in nearly all atmospheric diffusion experiments, whereas the time history measurements are relatively new. In both cases, the wake measurements were to be made directly within the cavity, rather than in the wake proper where the mean wind direction has been re-established.

The air flow within the cavity is unsteady, since each change in wind direction causes a new orientation of the building with respect to the prevailing wind, and thus a different equilibrium shape and position of the cavity. Winds within the cavity thus show a remarkable variability in direction at any given point, often going full circle in less than a minute. Since the efficiency of any sampler, whether aspirated or not, is a function of the relative direction of sampler port and wind direction (Green and Lane, 1957) and rapidly approaches zero when the wind is against the back of the sampler, some means of assuring wind flow into the face of the sampler was required.

The design evolved for the air samplers is shown in Figure 4. The air sampler itself is identical with that used in previous tests (Barad and Fuquay, 1962), a membrane filter aspirated by gasoline engine powered vacuum pumps through calibrated critical flow orifices. The samplers

1204929

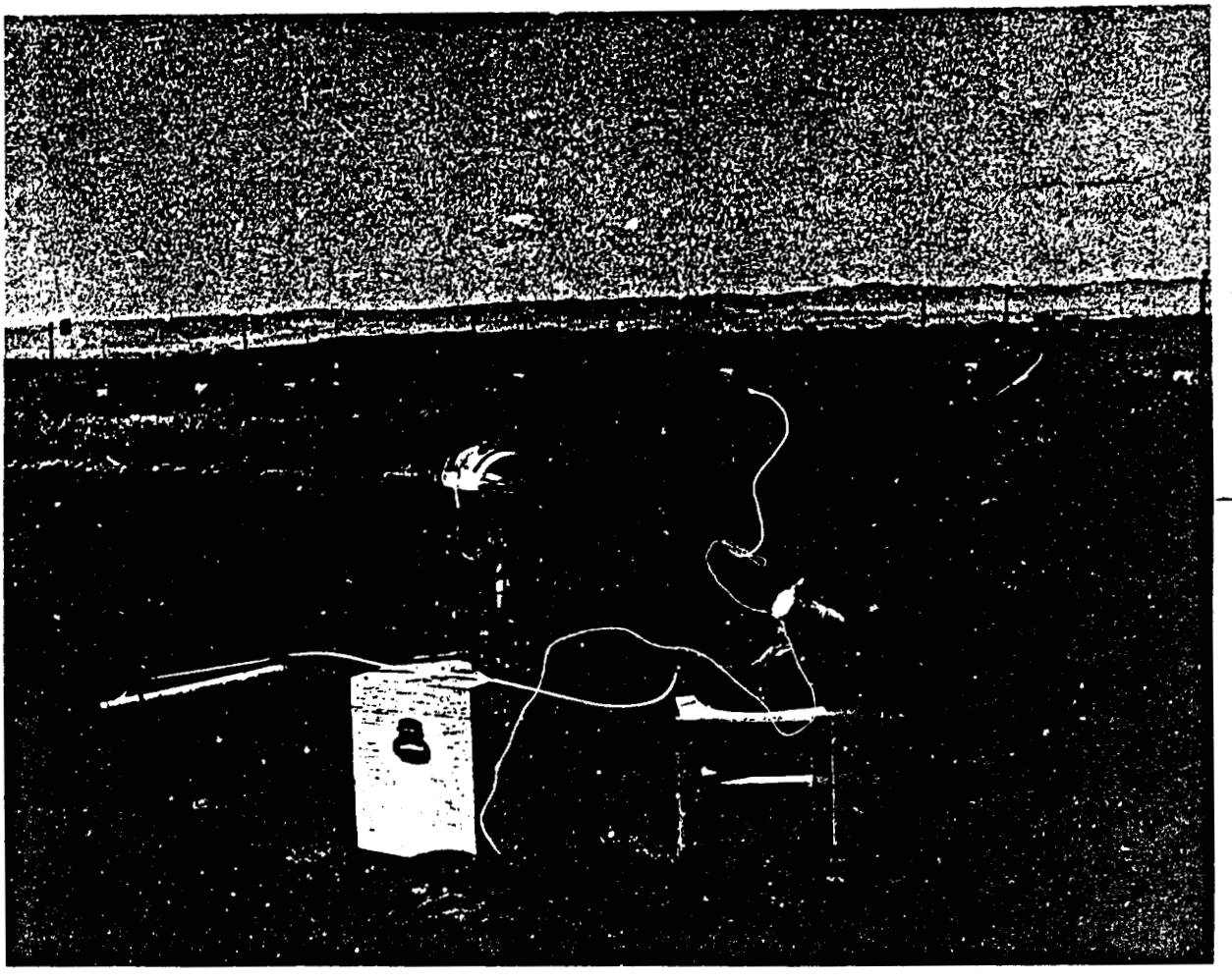

FIGURE 3. Tracer Dispenser and Associated Equipment

1204930

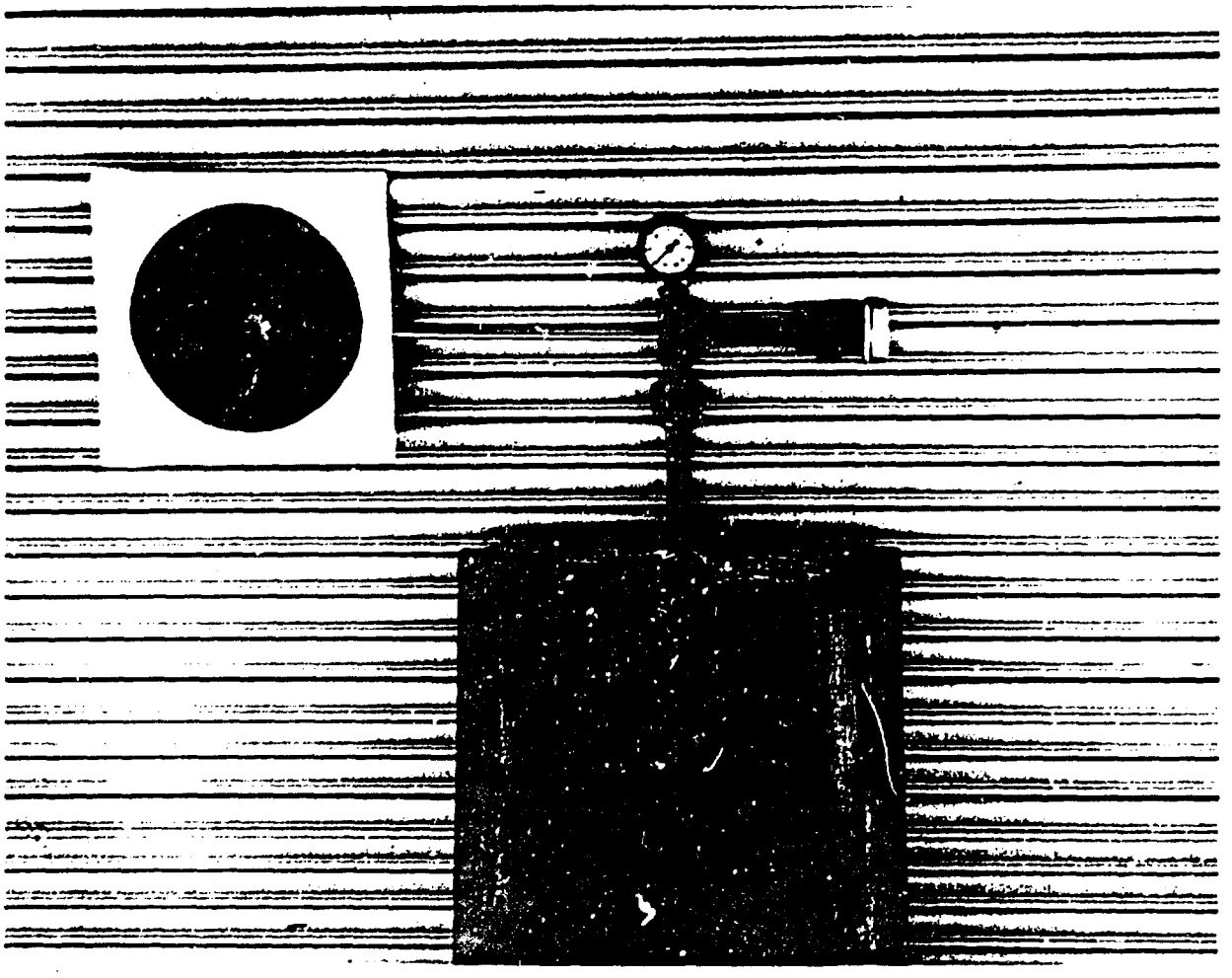

FIGURE 4. The Self-orienting Sampler

1204931

were mounted with a large tail to provide orientation with minimum overshoot and adequate turning moment in light winds, and dubbed SOS (Self-Orienting Sampler).

The measurement of time history of concentration was made with a Self-Orienting Real Time Sampler (SORTS), which is a Real Time Sampler (RTS) (Nickola et al., 1967) mounted with a tail similar to the SOS. The RTS uses the phosphorescence of ultraviolet irradiated zinc sulfide to activate a photomultiplier, and can reliably yield concentration measurements in the range from about 3×10^{-7} to 3×10^{-3} g/m^3. Although no precise measurement of the time constant of the RTS is available (or possible, since stationary sources of accurately known concentration are inordinately difficult to provide), it may be estimated by knowing the travel time through the sampler and the recorder speed. The time to traverse the sampler is about 0.8 seconds, and the full scale response time of the recorder is 0.5 seconds. Thus, to assure adequate accounting of instrument smoothing of the real concentration, average concentrations over five second periods were chosen as the minimum time resolution for data reduction. Figure 5 shows the SORTS*.

Other errors in sampling, such as anisokineticity and deposition were neglected. The anisokinetic error, which is due to air speed through the sampler being different than the ambient wind speed, results from curvature of streamlines near the sampler which finite particles may not follow due to their inertia. For the range of wind speed and particle sizes in this series, the anisokinetic error was not large, on the order of 20% at most, and probably about 10% in general (Sehmel,

*B. N. Nelson, Jr. of the Pacific Northwest Laboratory conceived and fabricated both the SOS and SORTS orientation system.

1204932

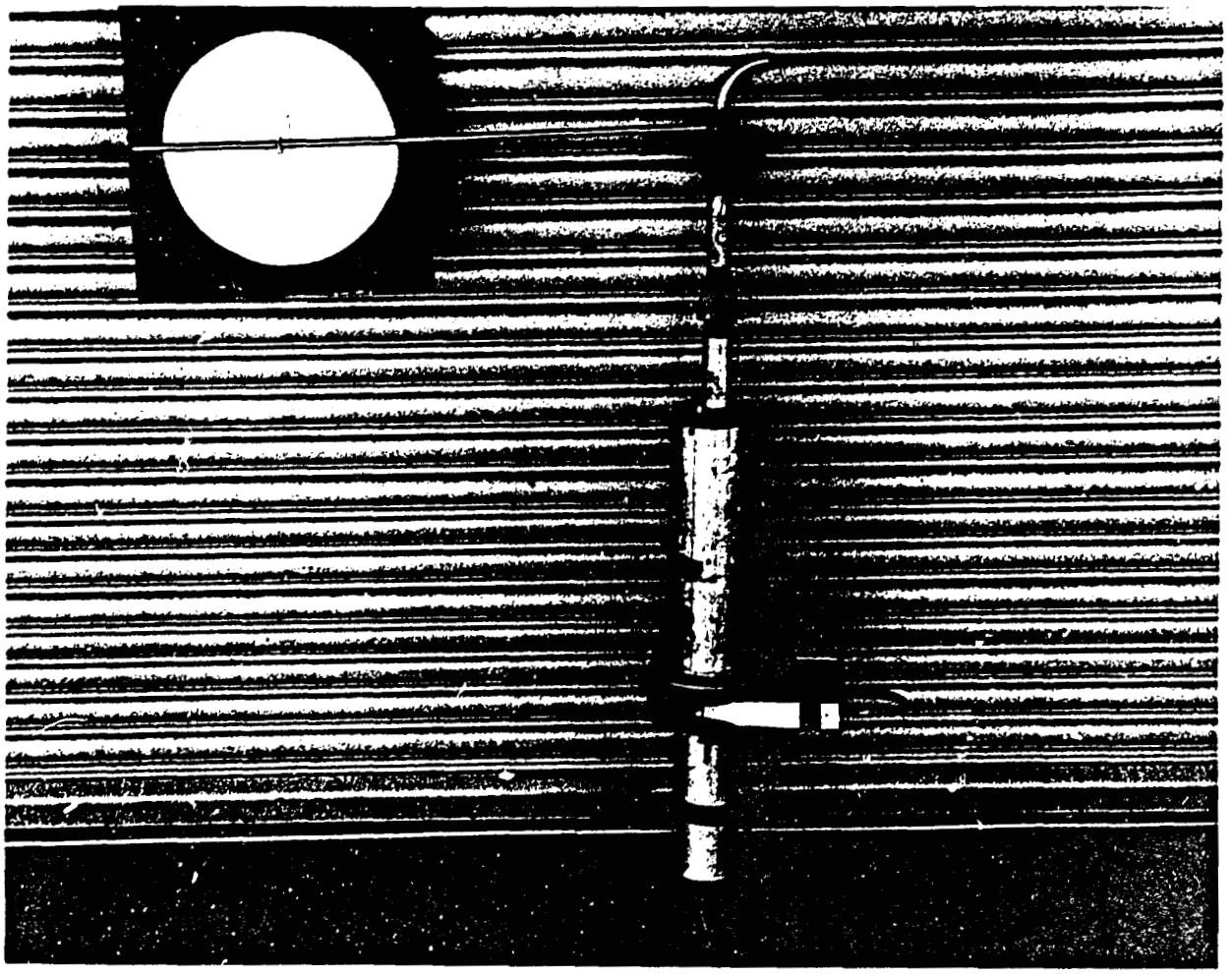

FIGURE 5. The Self-orienting Real Time Sampler

1204933

1966). Although deposition, the loss of tracer mass due to gravitational or eddy flux loss to the surface, can be large over long travel periods (Simpson, 1962; Islitzer, 1963), the short distances involved in this series did not allow time for large amounts to deposit.

Assay of the SOS samples was by use of the Rankin counter (Barad and Fuquay, 1962), which counts scintillations emitted from zinc sulfide when bombarded by alpha particles.

Design of the Sampling Grids

Two separate sampling grids were used in this study. One, the Control grid, was laid out around the Hanford 400 foot meteorological tower to indicate the history of concentration variation from an unobstructed point source. The second was laid out around a fairly large prismoidally shaped abandoned building to provide data showing the difference, if any, in concentration history in the lee of a building.

The Control grid consisted of three arcs of samplers at distances of 30, 50, and 100 meters from the source point. The arcs were 88 degrees in azimuth range, with samplers spaced 8 degrees apart; access roads allowed positioning of the SORTS near the center of the mean plume. To avoid introducing confusion, the SORTS was placed in position before tracer release and left stationary without regard to subsequent wind shifts. Figure 6 shows the Control grid from right angles to the test wind direction.

The Wake grid consisted of three arcs at 30, 50, and 100 meters from the center of a building 24 x 34 x 11 meters high. The arcs were considerably greater in angular coverage than the Control grid, due to the expected large shifts in wake positioning with wind direction

1204934

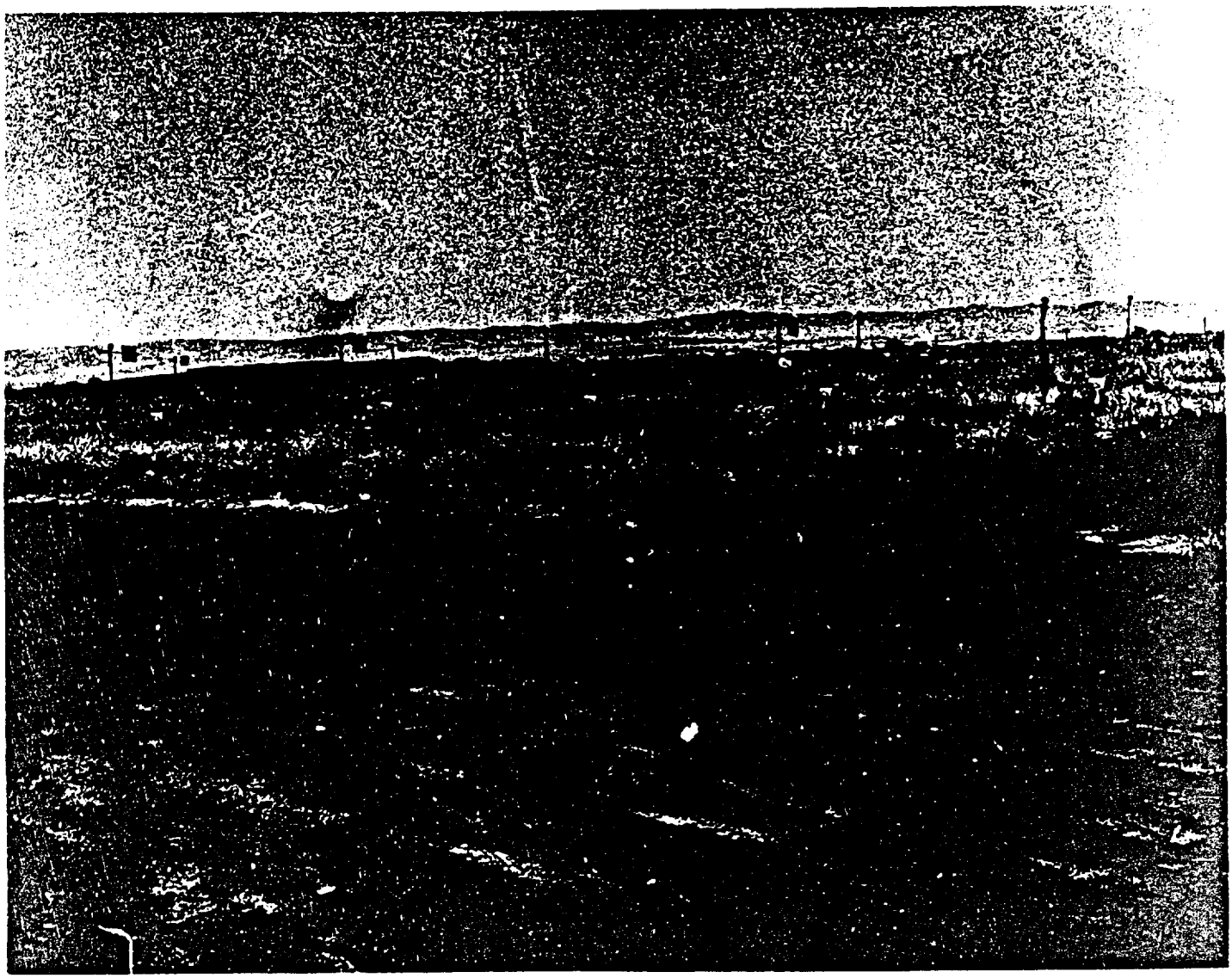

FIGURE 6. The Control Sampling Grid

1204935

changes. The inner arc covered 310 degrees, the middle arc 270, and the outer arc 200 degrees, with samplers spaced at 20 degree intervals. Figure 7 shows a portion of the Wake grid, looking essentially across the cavity area.

Field Procedure

The advent of favorable winds set the crew in motion, one man setting up and checking out the generator and preparing the tracer formulation, another to starting the sampler engines, and a third to placing filters in the SOS samplers. The operator of the SORTS was tentatively stationed downwind where calibration and checks were completed. Usually within an hour the final position of the SORTS was chosen, and tracer release was begun. Due to the small size of the formulation container, only short-term tests could be attempted in this series, and tracer release usually was restricted to 10 or 15 minutes.

The SORTS recorder was run at a chart speed of six inches per minute, so the (mechanical) integrator was read in increments over half inches, a simple task, to yield average concentrations over five-second intervals.

1204936

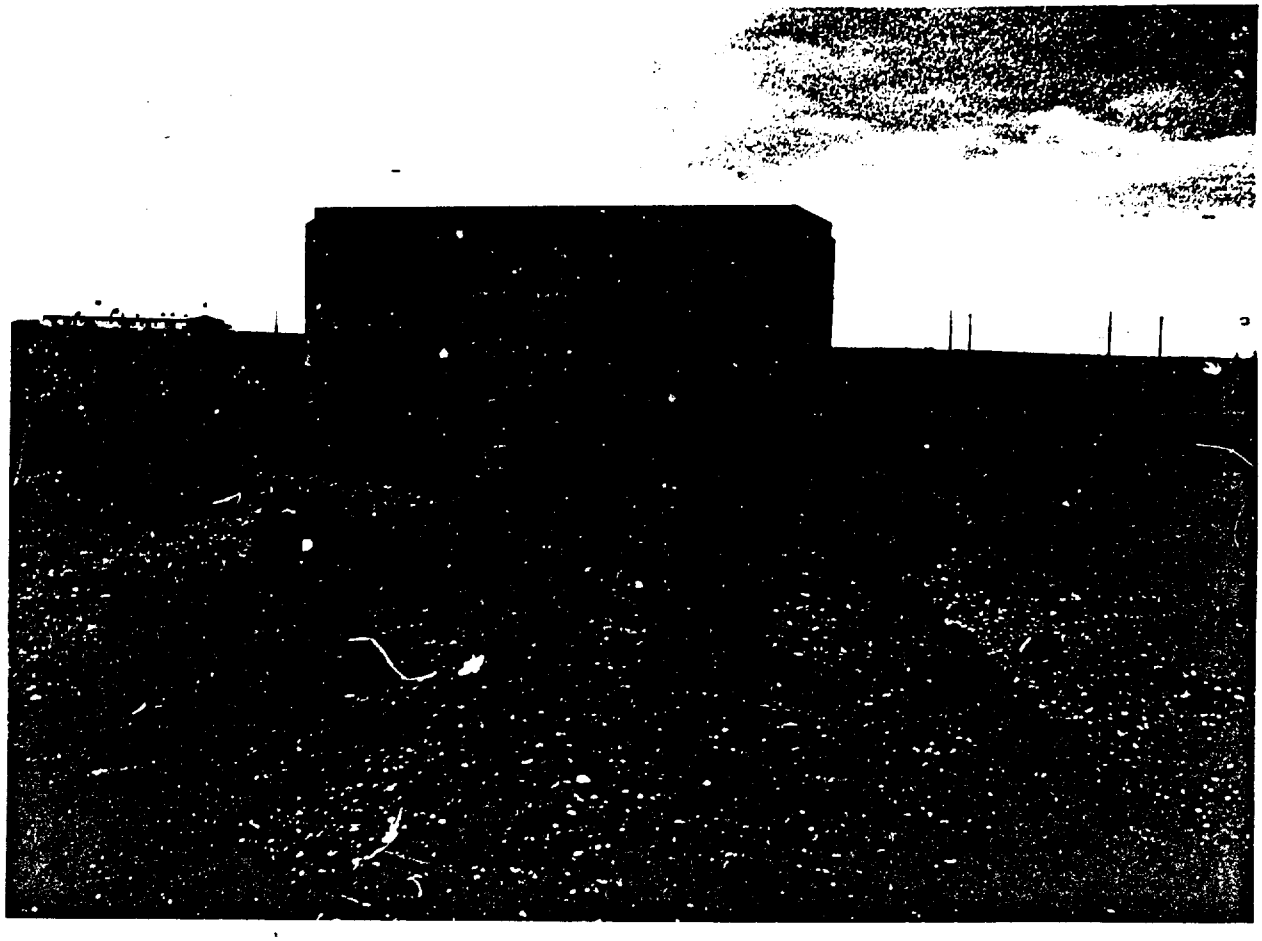

FIGURE 7. The Wake Sampling Grid

1204937

CHAPTER THREE

DATA REDUCTION AND PRESENTATION

The data gathered in this series of diffusion experiments consisted only of concentration measurements. This is a rather unusual situation for meteorological tasks, and should be explained. The most important factor was logistical in nature; although fairly sophisticated meteorological measurements were readily available for the Control tests, only the most gross measurements were possible for the Wake test, since no portable instrumentation was available. Since the variance of concentration was to be investigated, there was little point in measuring only mean wind over the period of testing; any useful information must surely come from the variance of wind speed or direction. However, the governing equation derived in Chapter One is independent of meteorological parameters, depending only upon the time history of concentration, so no need for wind or temperature measurements was introduced. Furthermore, to investigate whether first order difference in concentration variability were introduced by the presence of a large obstacle, the direct measurement of concentration rather than air flow parameters is the more desirable. Therefore, rather than distract from the investigation of concentration per se by attempting to correlate results with mean atmospheric conditions, a procedure which is increasingly questioned (Pasquill, 1963), no wind or temperature data were recorded.

The decision to divorce the Wake and Control tests from atmospheric conditions was not made hastily. Martin's work (1965) strongly indicated that in wakes the presence of aerodynamically produced turbulence

1204938

overshadowed effects of atmospheric stability or wind conditions so long as the wind was strong enough to produce a wake, say five meters per second. This is particularly true in the cavity, since even very strong stability, or very strong winds, are disrupted entirely due to the increased turbulence intensity. There was thus no necessity for atmospheric conditions to be known in detail.

Mean Concentration Patterns

The average concentration patterns as shown by the SOS grid were used to illustrate the position of the SORTS with respect to the source and were not required for other work, so the patterns are given in arbitrary units.

Figures 8 and 9 present the mean concentration isopleths for the Control tests C-3 and C-4. Note that the patterns are both slightly bimodal. The SORTS was situated as nearly due downwind as was possible to forecast, as indicated on the figures.

The patterns from the Wake tests are shown in Figures 10 and 11 for Tests W-6 and W-7, respectively. Although the source point, indicated on the figures, was placed at an upwind corner, still an asymmetrical concentration pattern resulted. This is probably a reflection of the mean wind being slightly off the corner; since a point source was used, effectively only a single streamline was traced near the source.

Time History of Concentration

In an appendix, the concentration recorded by the SORTS is given for each of the tests. The tabled data are five-second averages of concentration, normalized to the mean at the SORTS position.

1204939

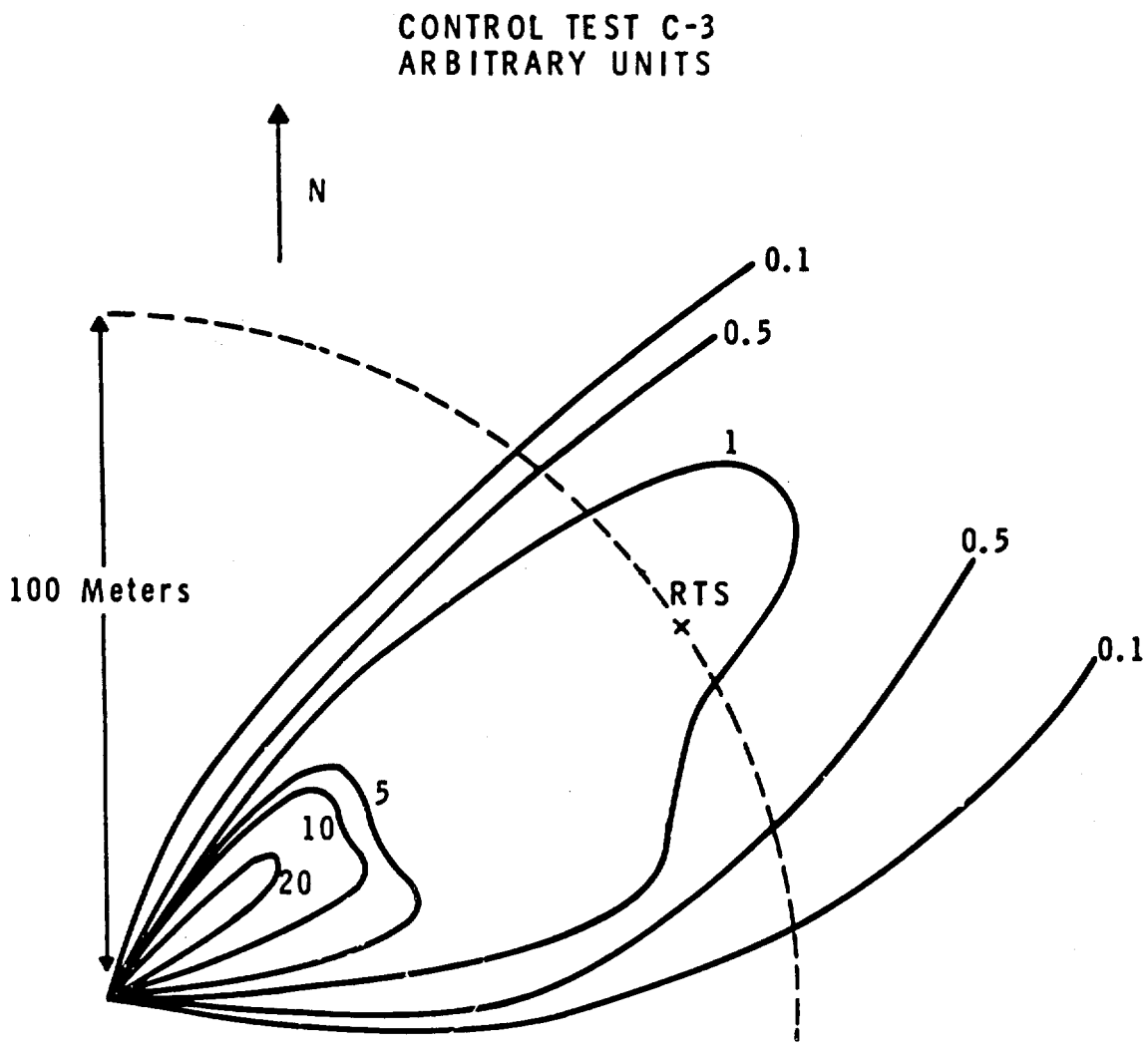

Figure 8
Mean Concentration Isopleths for Control Test C-3

1204940

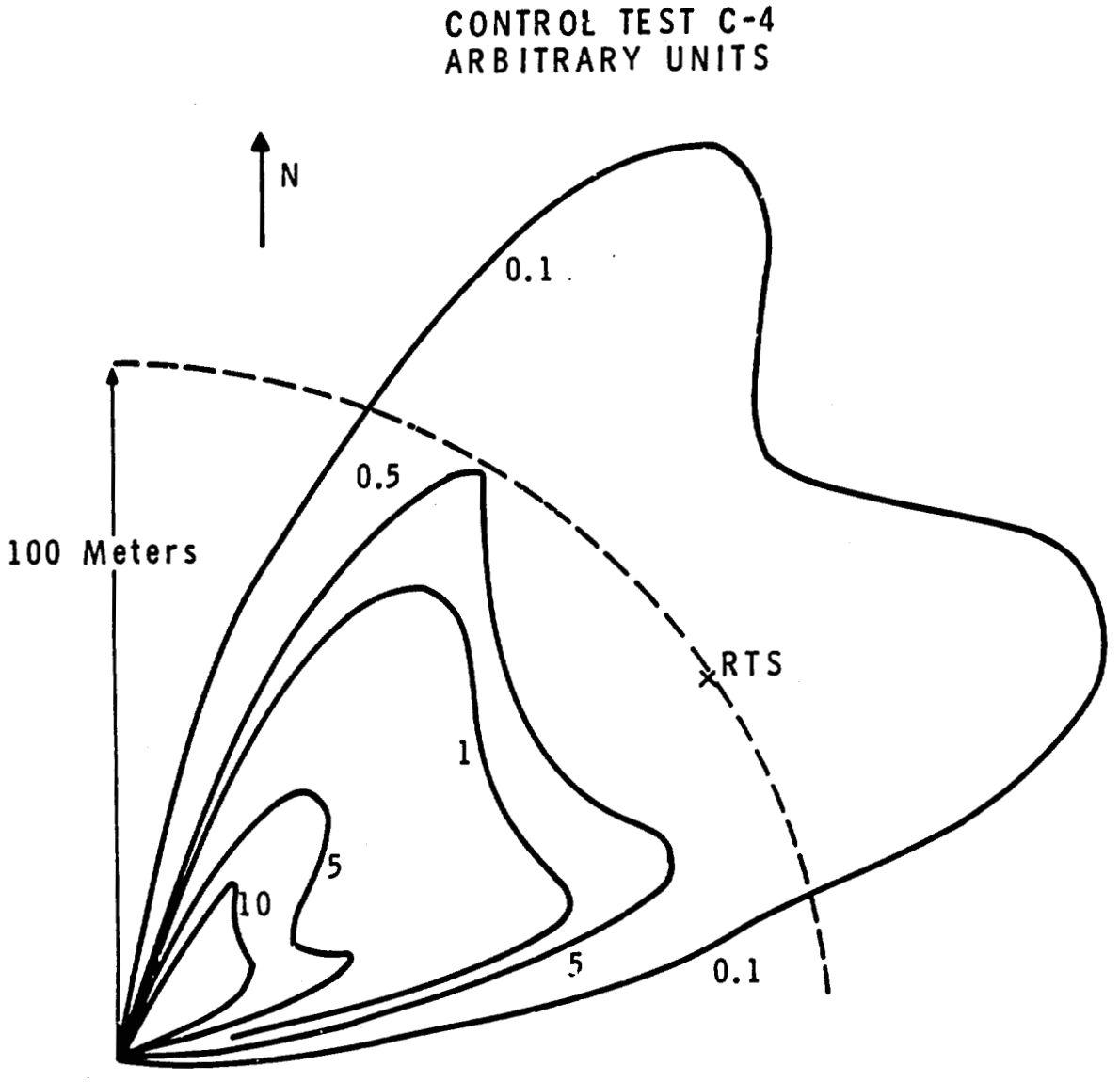

Figure 9
Mean Concentration Isopleths for Control Test
C-4

1204941

WAKE TEST W-6
ARBITRARY UNITS

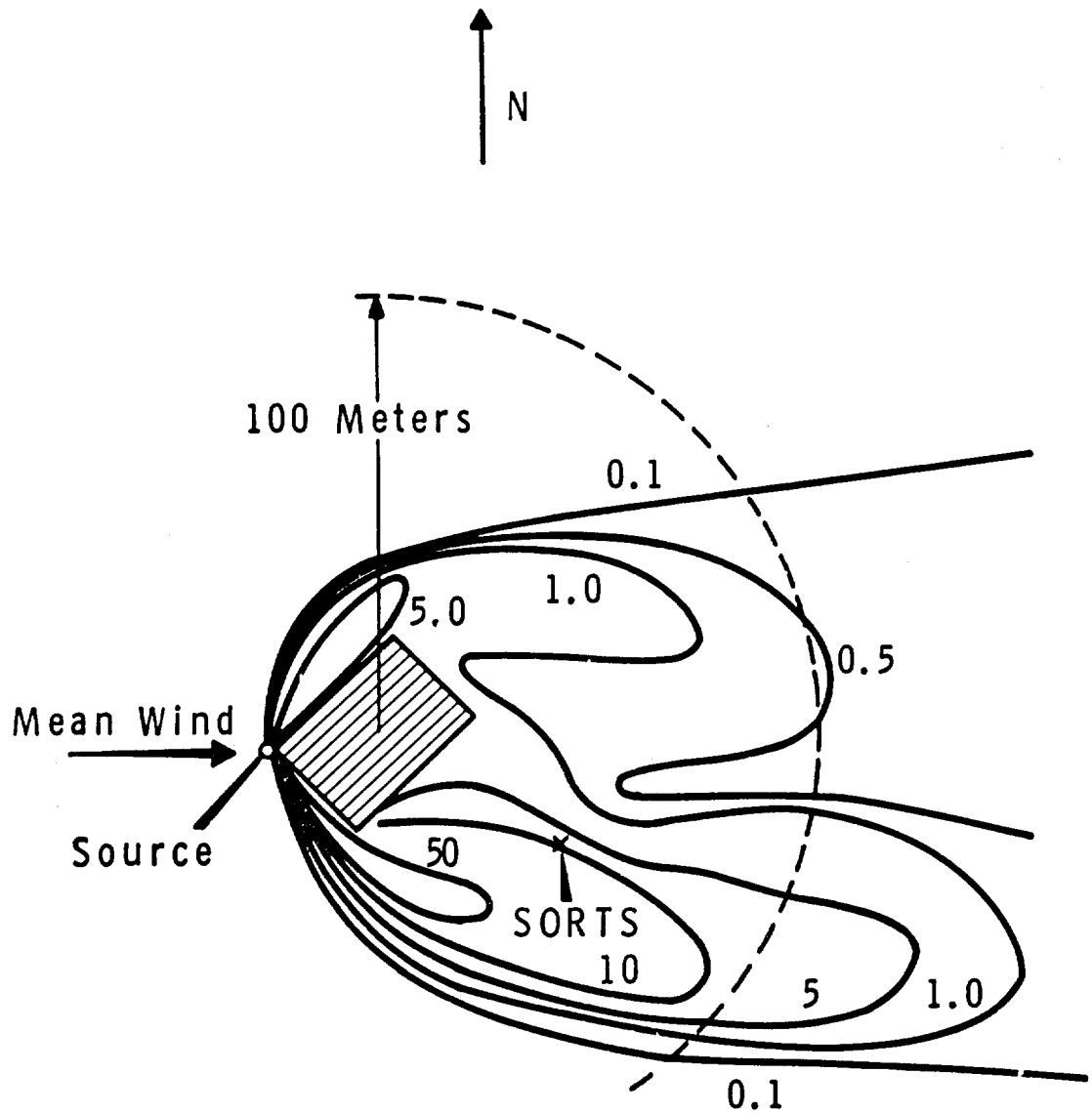

Figure 10
Mean Concentration Isopleths for Wake Test
W-6

1204942

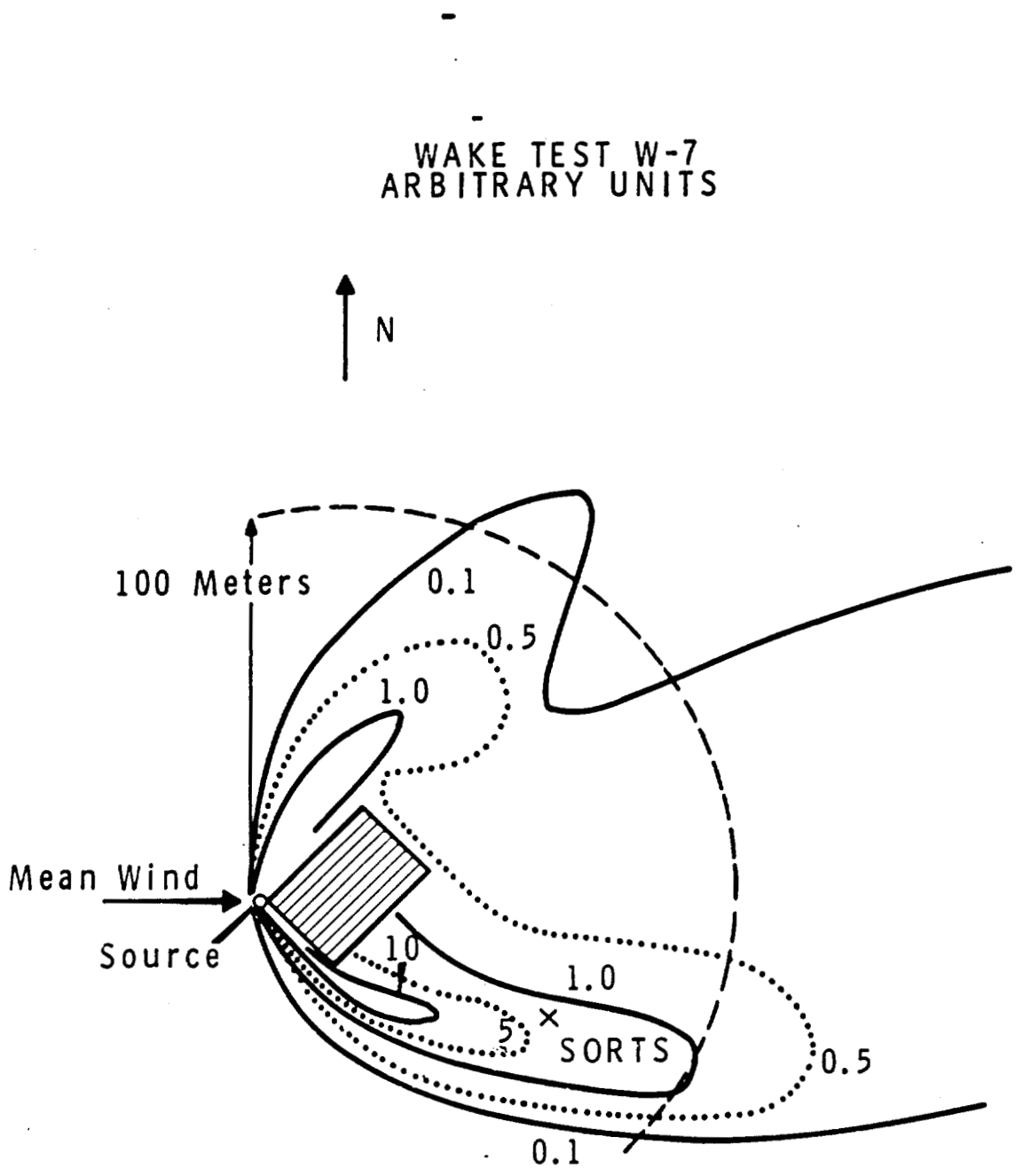

Figure 11
Mean Concentration Isopleths for Wake Test
W-7

1204943

CHAPTER FOUR

DATA ANALYSIS

Several points investigated using the data gathered during the four tests are discussed here. First, some idea of the distributions of concentration at a point is given. The data derived from increasingly smoothing the concentration trace are then compared to the theoretical forms derived in Chapter One. Finally, the peak-to-mean ratios observed in wakes and point source plumes are examined and compared.

Distribution of Observed Concentrations

Although not nearly enough tests have been completed for a definitive test of the distribution of concentration observed at a point, some guidance concerning what may be expected is certainly possible. It has been assumed on occasion that the time distribution of concentration is akin to a Poisson distribution, more for convenience than rigor (Csanady, 1967). The Poisson distribution itself is incorrect in principle, since each of the observations forming a Poisson distribution must have the same expected value, a condition which is obviously in conflict with the finite memory of the atmosphere embodied in the finite time scale of autocorrelations.

If, in fact, the distribution were Poisson, the variance and mean of the distribution would be identical. Table I shows the observed values of the variance and the mean; clearly the strict Poisson distribution is inapplicable. However, the standard deviation and the mean are approximately equal, a phenomenon which has been reported for tube flow also (Csanady, 1967).

1204944

TABLE I

Test	Mean	Variance	Standard Deviation
C-3	0.656×10^{-4}	0.878×10^{-8}	0.937×10^{-4}
C-4	0.310×10^{-4}	0.358×10^{-8}	0.598×10^{-4}
W-6	4.83×10^{-4}	167.0×10^{-8}	12.9×10^{-4}
W-7	0.817×10^{-4}	0.760×10^{-8}	0.872×10^{-4}

The frequency polygons of concentration observations are presented in Figure 12. Three of the tests are rather comparable in distribution, but W-7 is anomalous in appearance. Since W-7 was a very short test (6 minutes), it may well be that the distribution is not stable — that a considerable proportion of variability was yet to be evidenced in the length of record. It should be noticed that all the tests show a decided upturn at low values of $\chi/\overline{\chi}$. This tendency is more clearly shown in Figure 13, the composite of all four tests. The increase in frequency of low values of $\chi/\overline{\chi}$ is a clear indication of the importance of intermittency in concentration fluctuations even near the centerline.

Variance of Concentration

Any attempts to compare the theoretical forms discussed in Chapter One with the data described in Chapter Three should begin by calculating the parameters b and k directly from covariance data. However, such calculations were not at all successful. A variety of problems seem to accumulate during such calculations, mostly concerned with the lack of knowledge of the variance and autocovariance of the unsmoothed function. Clearly, the character of the unsmoothed function becomes crucial as t,

1204945

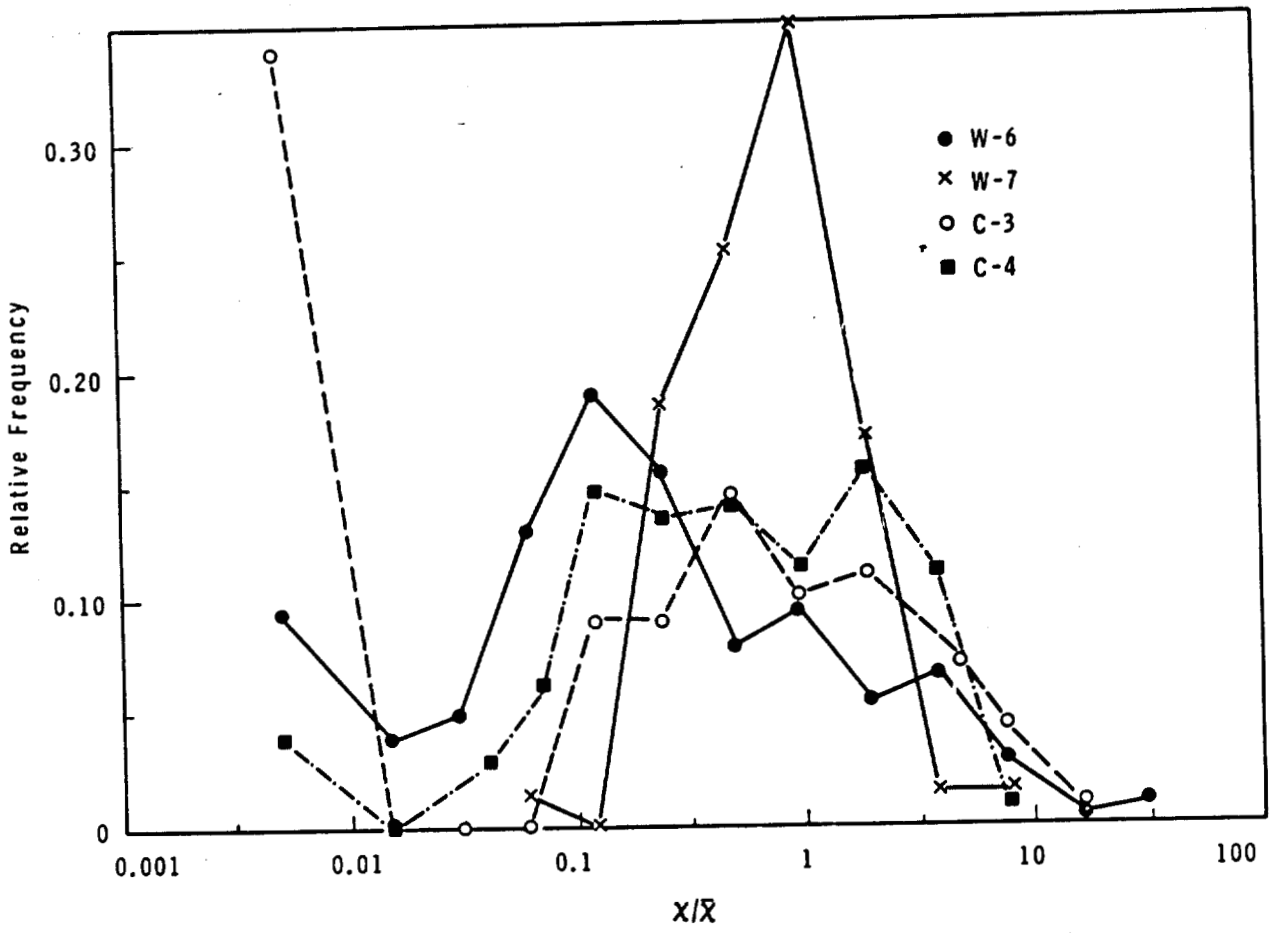

Figure 12
Frequency Distributions of Concentration Ratio
$x/\bar{x}$

1204946

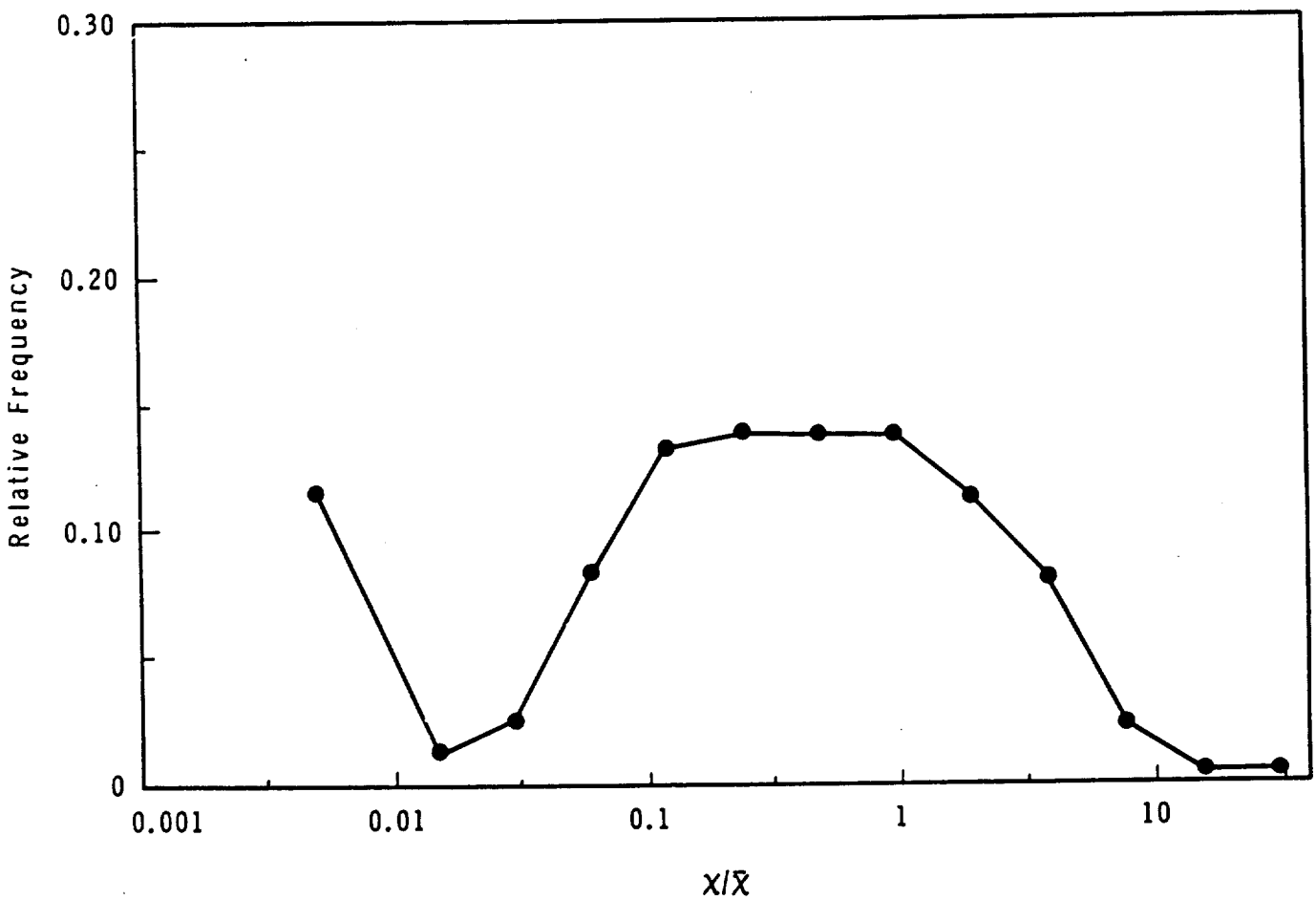

Figure 13
Composite Frequency Distribution of
Concentration Ratio $\chi/\bar{\chi}$

1204947

the smoothing interval, approaches zero. Since it is at or very near $t = 0$ that b can be calculated, it is not surprising that estimates of b are not accurate. On the other hand, k is determined by approximating the area under the autocovariance function, which is a function of the covariance at t near zero, also; hence, k depends upon knowledge of b, so neither parameter can be well estimated.

Alternate checks of the theory against data are possible, however. First, b and k can be experimentally determined by, respectively, the slope of $\sigma_s^2/\sigma_{s,o}^2$ near $t/t_o = 1$, and by the displacement of the data from a power law at some large t/t_o, say 20 or 40. If the approximations are accurate, the curve generated with these values of b and k should fit the data at all other t/t_o. Also, using the calculated values of b and k, the observed autocovariance function can be compared to the function calculated from $P'(t/2) = \frac{1}{2}(2+b+kt)\,\sigma_s^2$, where $P'(t/2)$ is an estimate of the autocovariance as a function of lag time t. If the approximations are accurate, $P'(t/2)$ should correctly reflect the observed covariance in a smoothed fashion.

The results of the first comparison are shown in Figures 14 and 15, for the Control tests, and 16 and 17 for the Wake tests; the corresponding values of b and k are given in Table II. The agreement between theory and data is good, and by slight alteration in the values of b and k, would be made better. The illustrated fit was chosen to point out a regularity in the values of b as a function of release time. Further evidence of b increasing as length of record increases is presented by Hinds (1968), where a record of crosswind turbulent fluctuations for one hour yields $b \approx -1/6$, and Islitzer (1963), who indicated one and

1204948

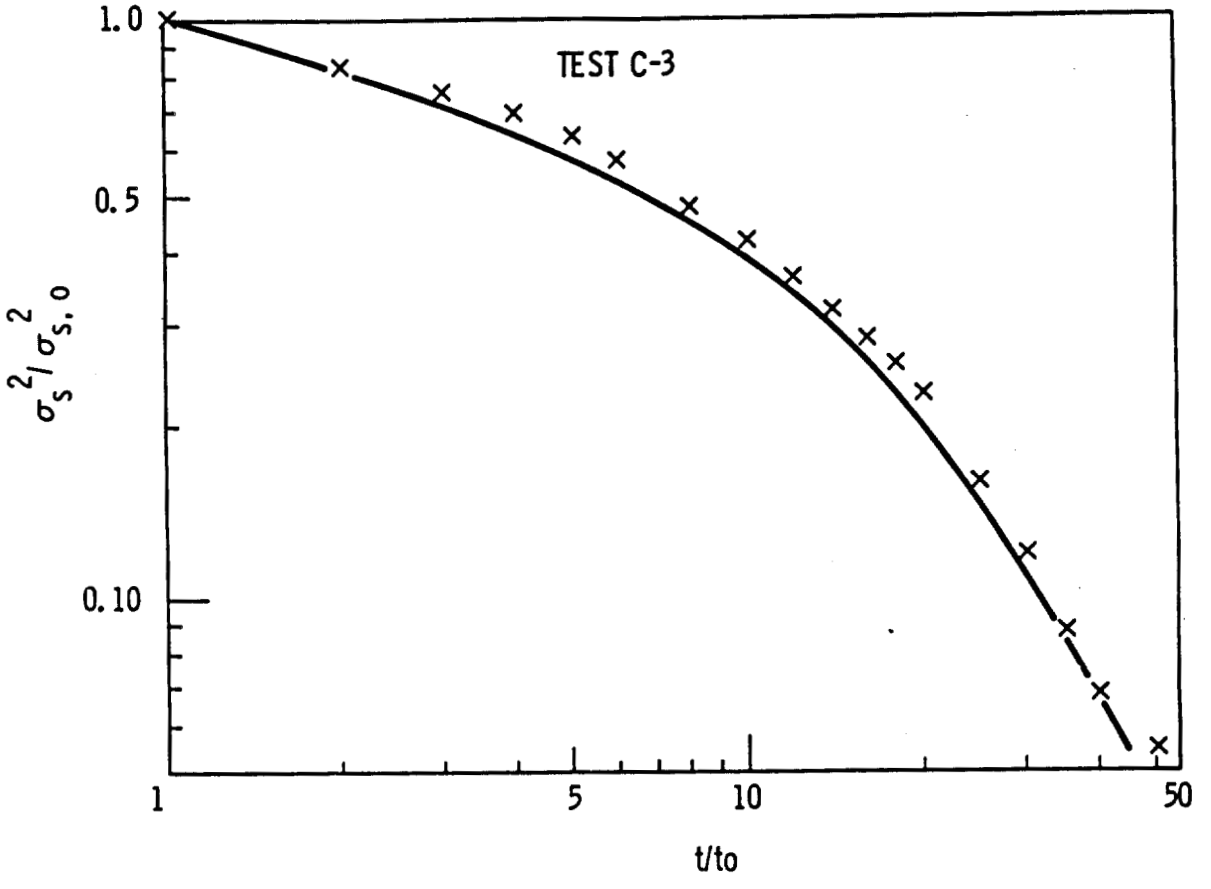

FIGURE 14
Fractional Decrease in Variance with Increasing
Smoothing Interval, Control Test C-3

1204949

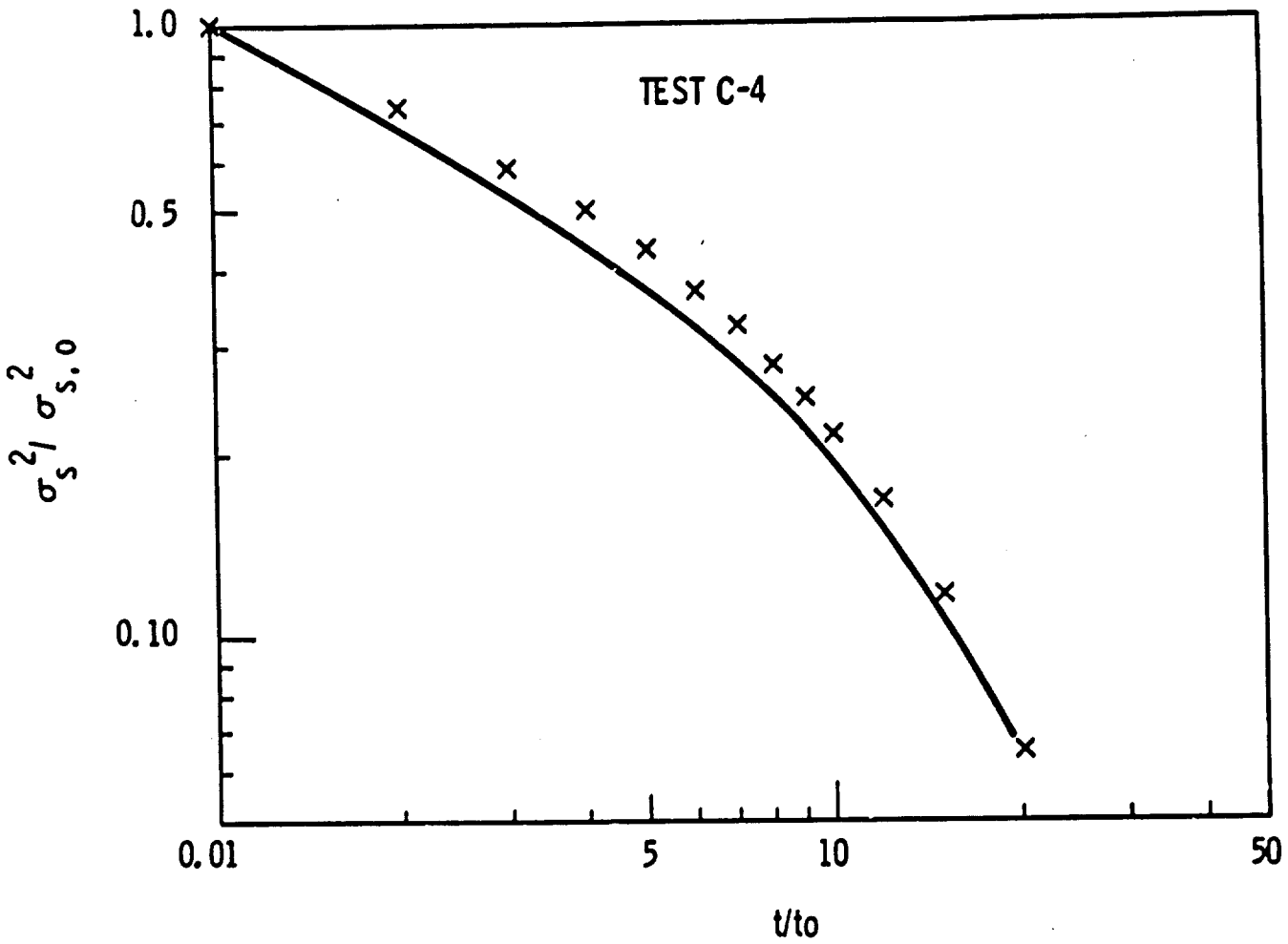

Figure 15
Fractional Decrease in Variance With Increasing Smoothing Interval, Control Test C-4

1204950

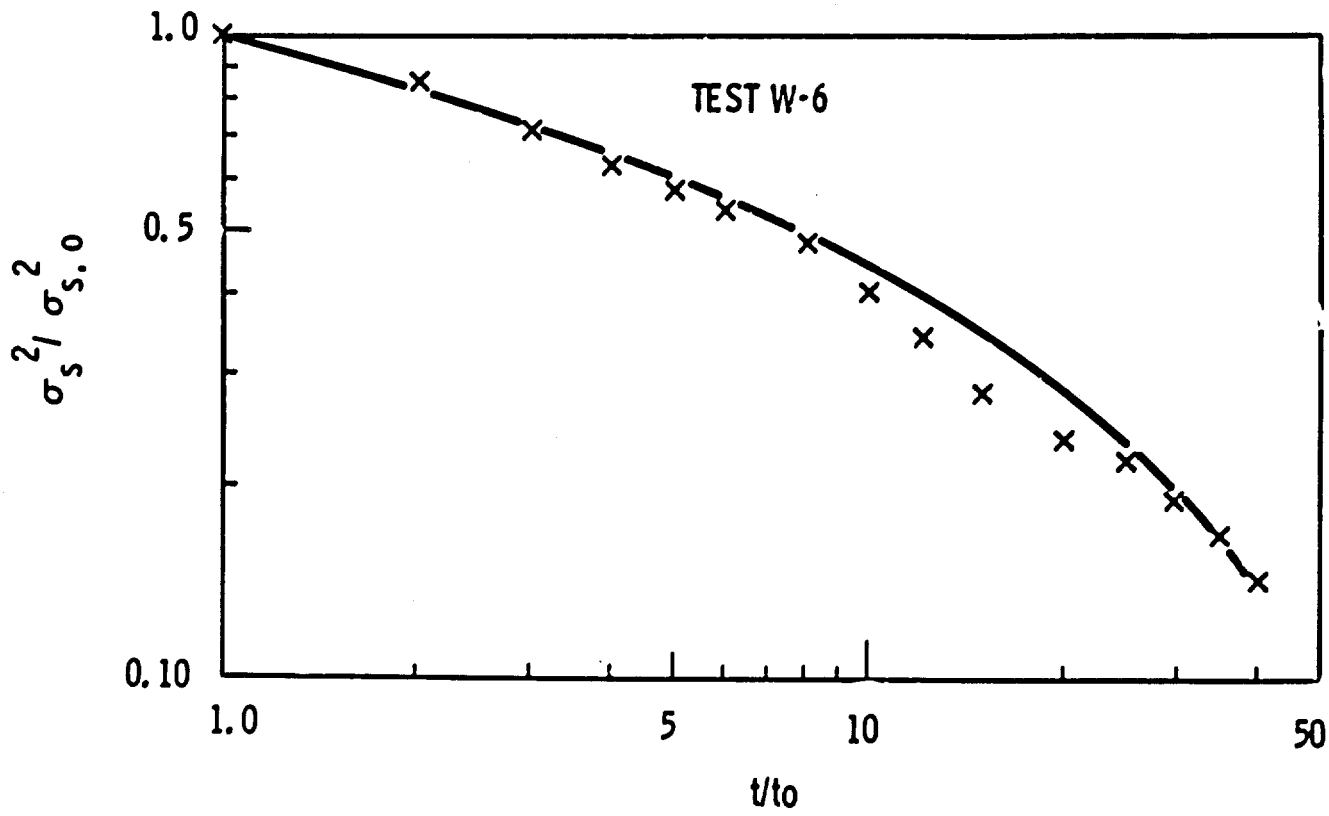

Figure 16
Fractional Decrease in Variance With Increasing
Smoothing Interval, Wake Test W-6

1204951

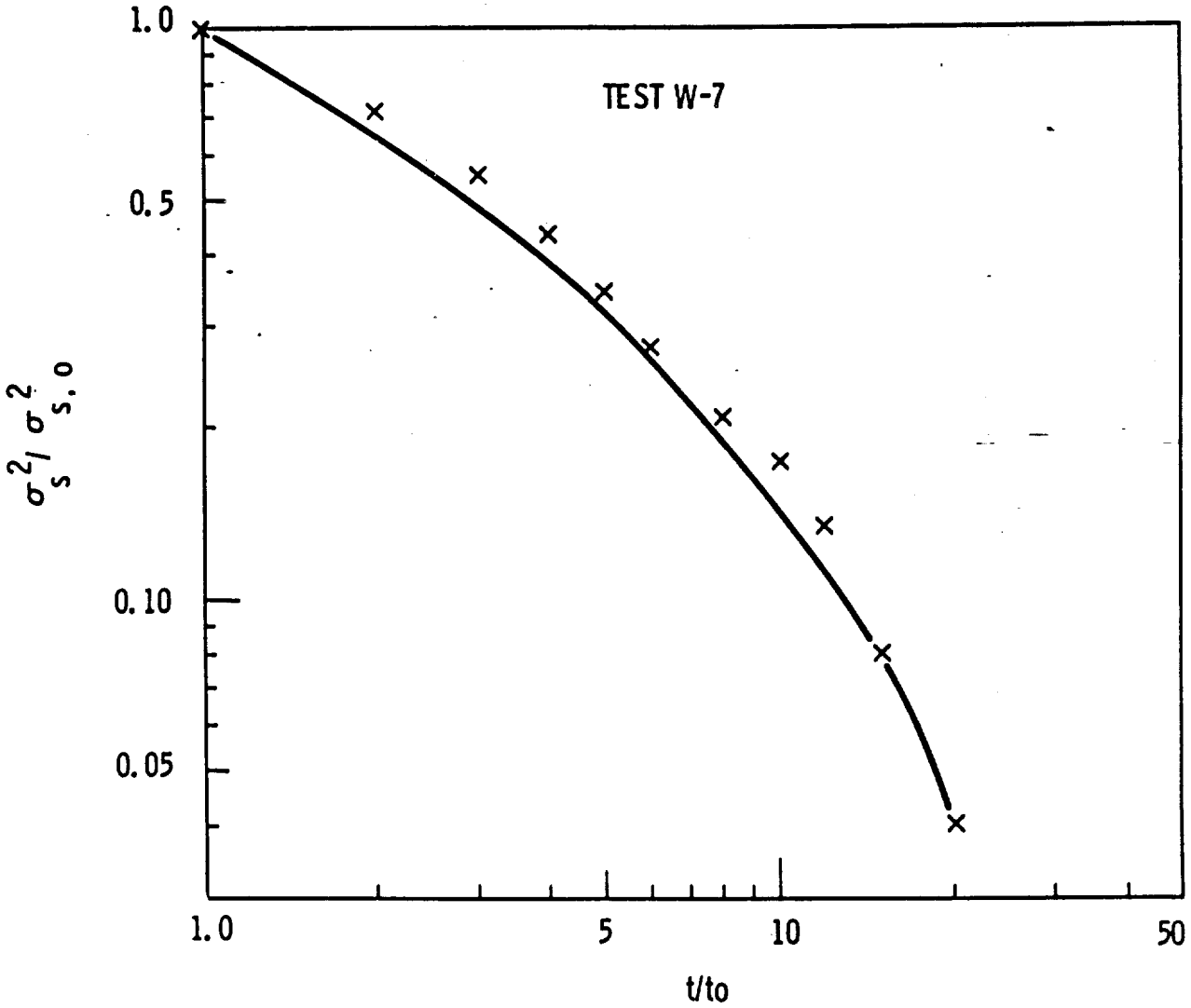

FIGURE 17
Fractional Decrease in Variance With Increasing Smoothing Interval, Wake Test W-7

1204952

two hour records of wind direction yield $b \approx -1/8$ and $-1/16$, respectively.

TABLE II

Test	b	k
C-3	- 1/4	- 0.0090
C-4	- 1/2	- 0.0130
W-6	- 1/4	- 0.0053
W 7	- 1/2	- 0.0181

The results of calculating $P'(t/2)$ from b and k are presented in Figures 18 and 19 for the Control tests and 20 and 21 for the Wake tests. Although the observed detail is not evident in the calculations, the scale is rather accurately estimated. Note that the linear approximation in Equation 20 does not imply a linear autocovariance, due to the appearance of σ_s^2, a nonlinear parameter.

The solution following from Equation 19, which assumed an exponential form for the quasi-autocorrelation $P(t/2)/\sigma_s^2$, is awkward to work with, due to the slowly converging nature of the series. However, calculations from it also fit the data reasonably well, as shown in Figure 22. Here only two terms in the series have been used, so the useful extent of t/t_o is smaller than in Figures 14 through 17.

Peak-to-Mean Concentration Ratios

There are several manners in which peak-to-mean ratios may be presented. Perhaps the most informative is that used by Gifford (1960) in one of his figures. He presented the peak-to-mean ratios as a function of total time of data collection divided by the period of averaging.

1204953

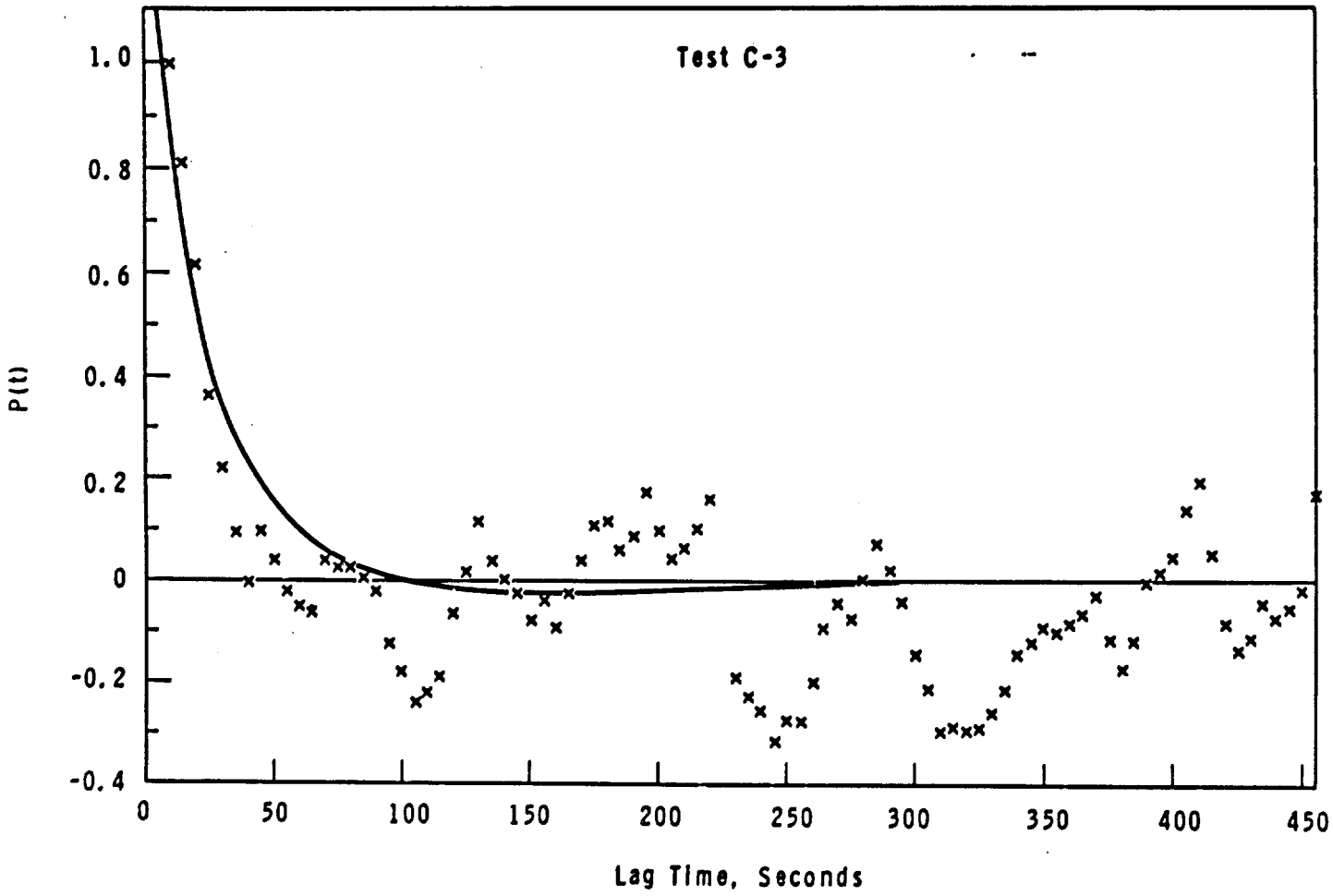

Figure 18
Calculated and Observed Autocovariance Function
Control Test C-3

1204954

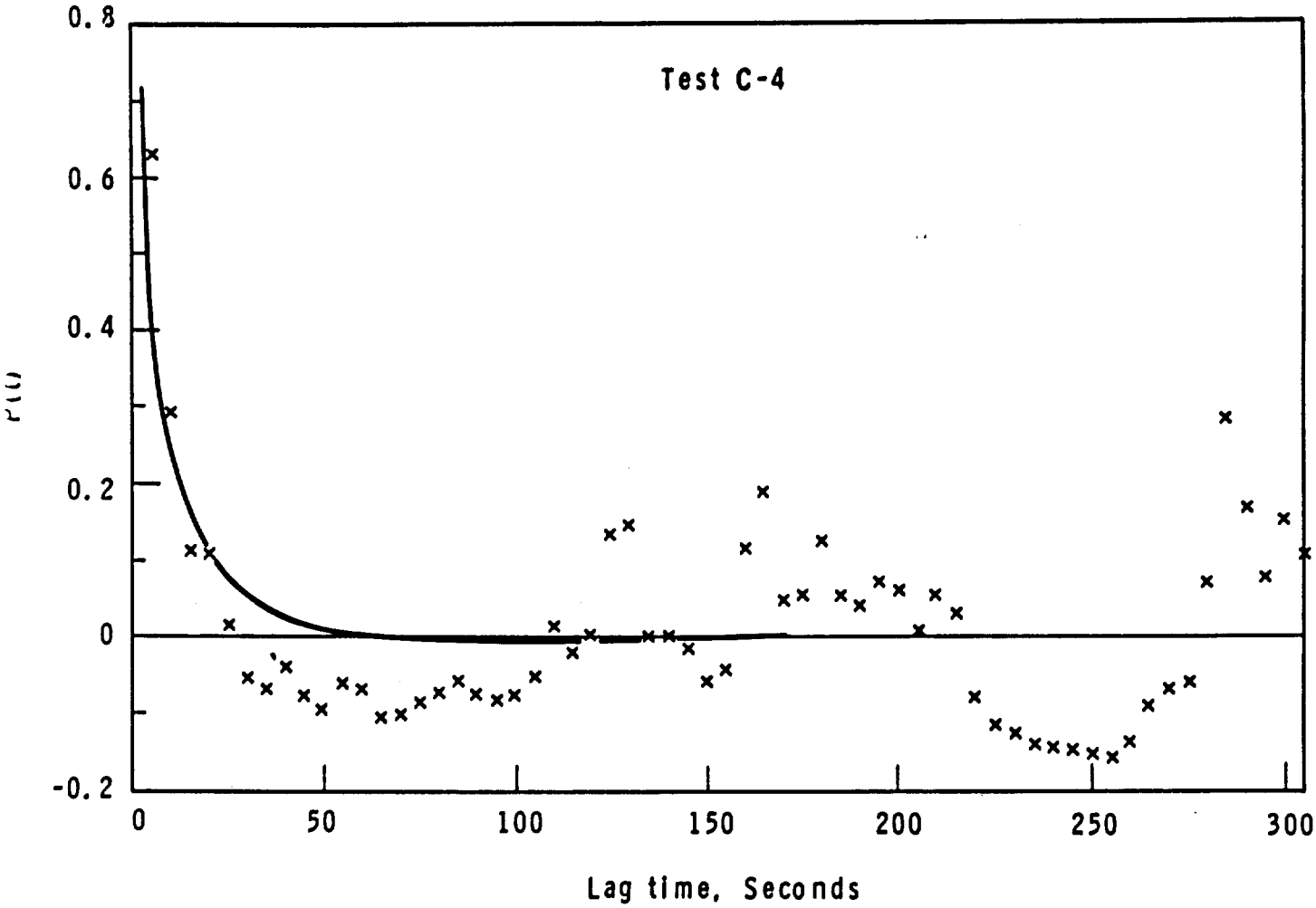

Figure 19
Calculated and Observed Autocovariance Function
Control Test C-4

1204955

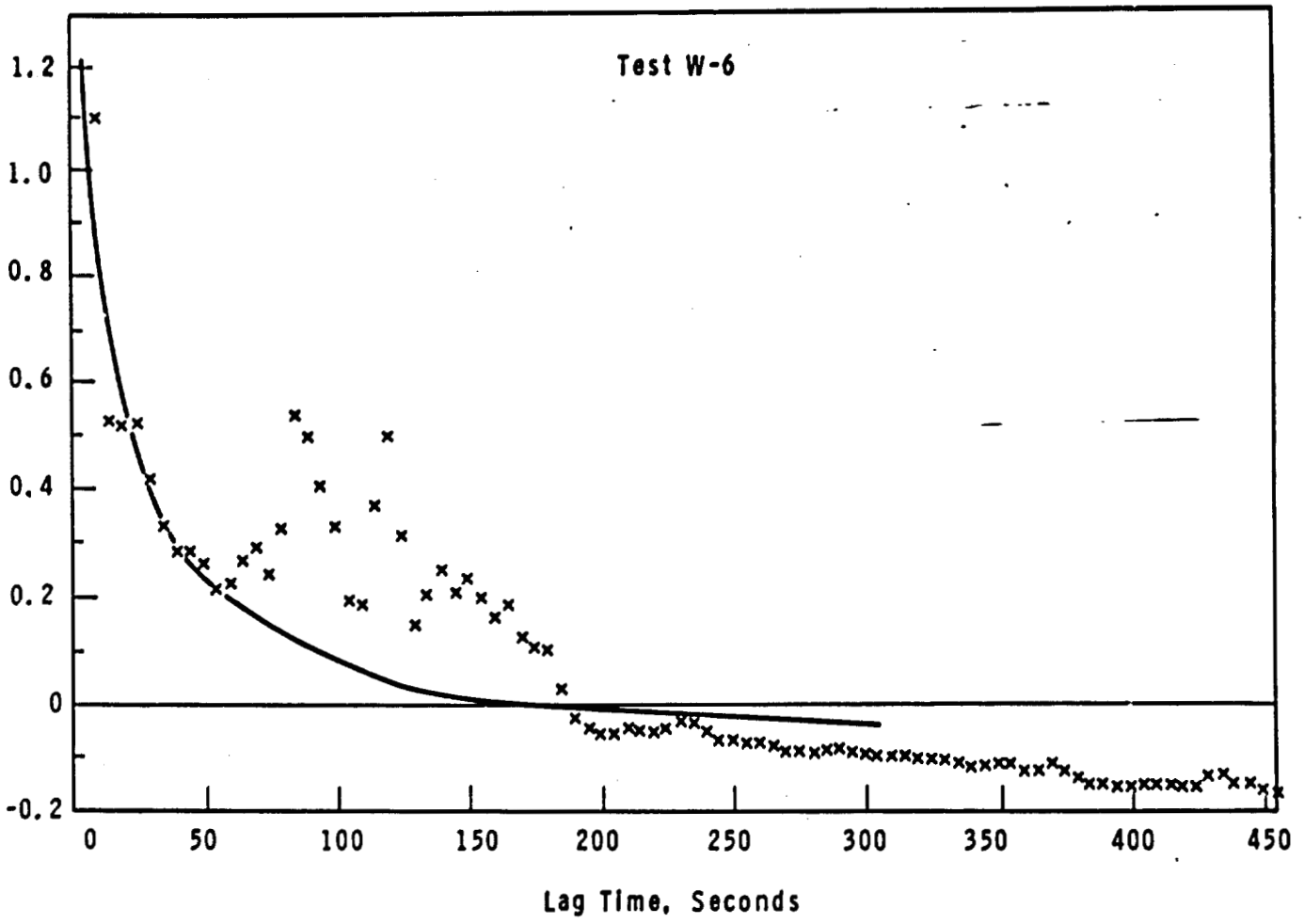

Figure 20
Calculated and Observed Autocovariance Function
Wake Test W-6

1204956

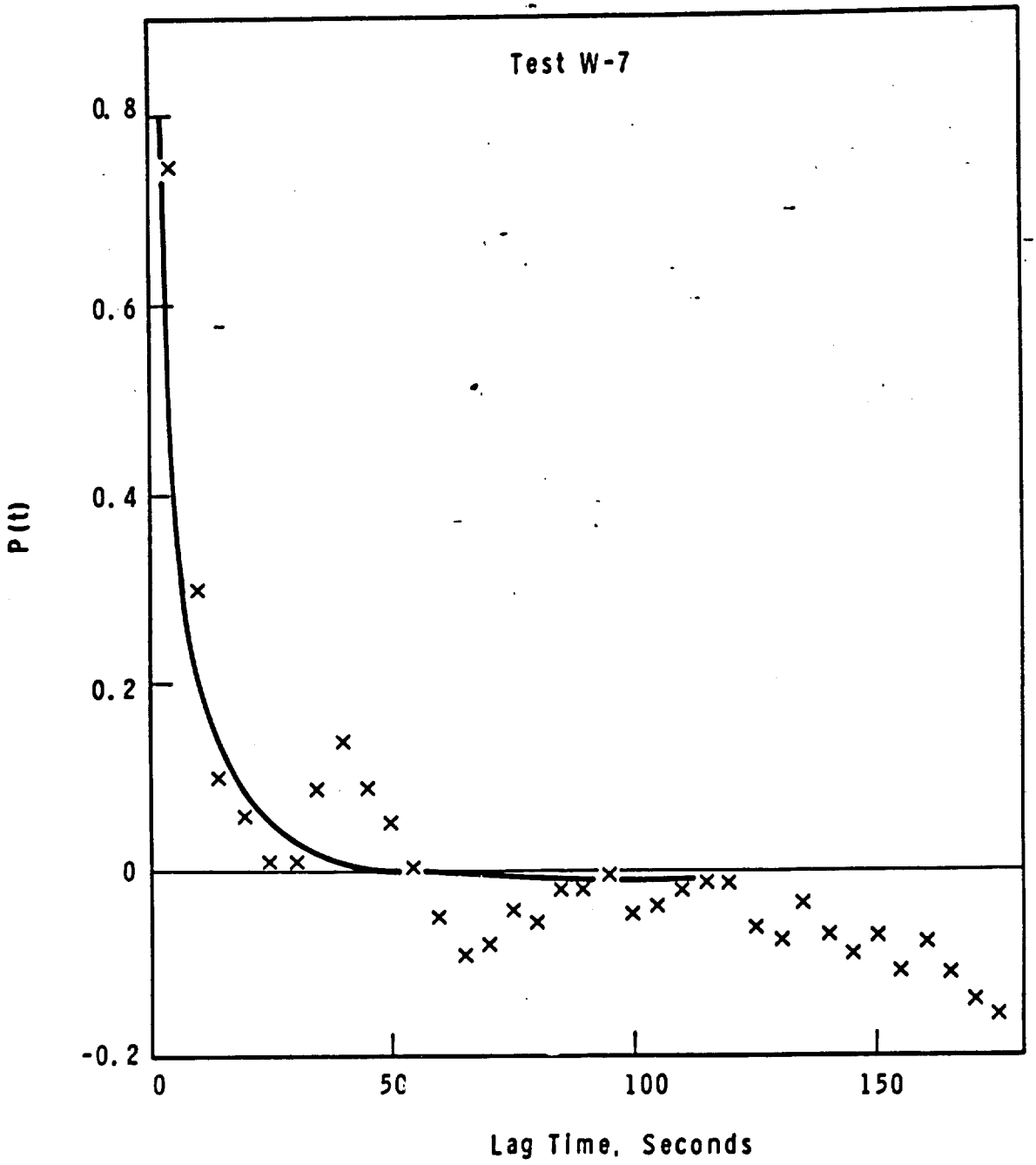

Figure 21
Calculated and Observed Autocovariance Function
Wake Test W-7

1204957

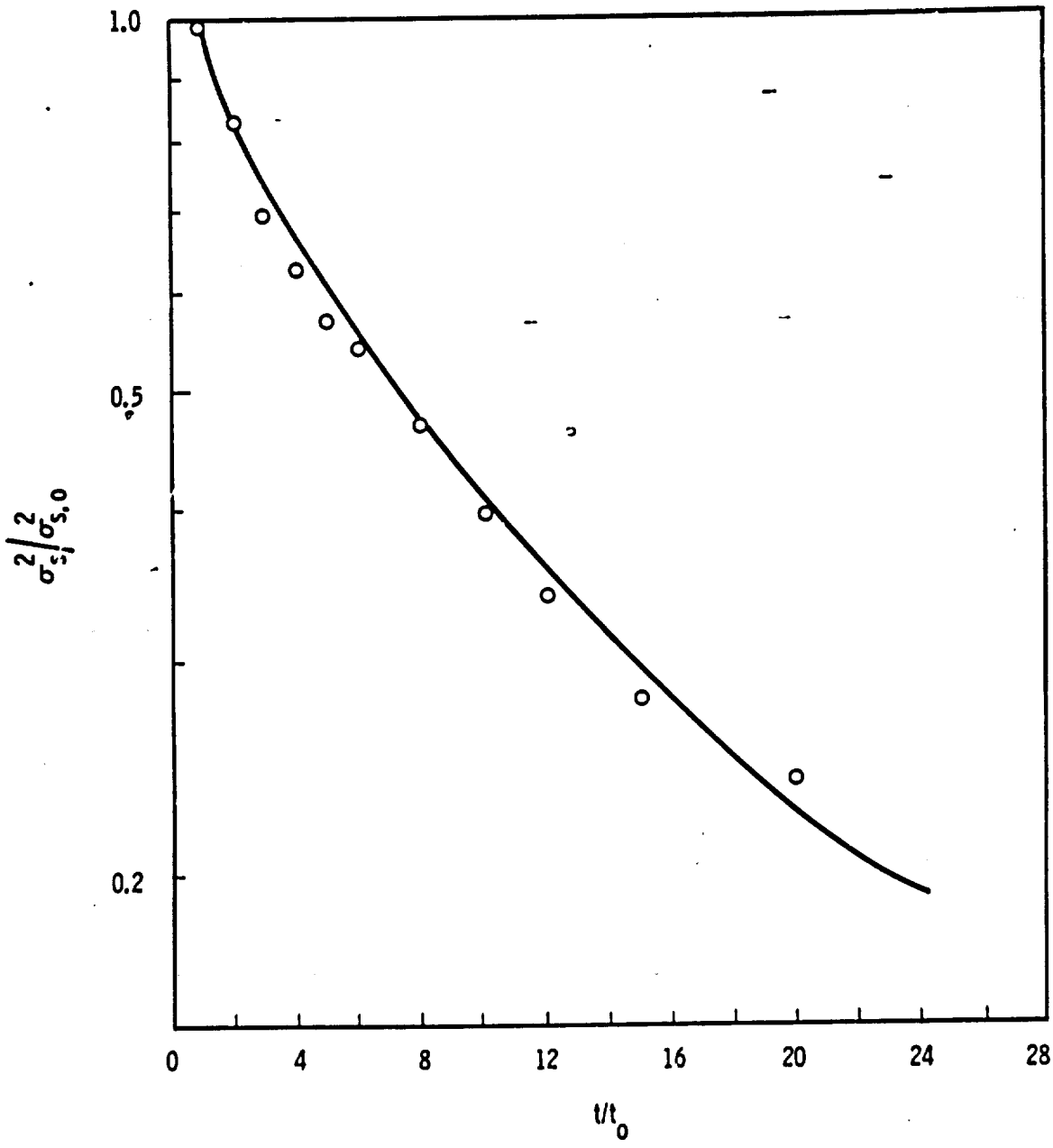

Figure 22
Fractional Decrease in Variance vs Smoothing Interval With Exponential Form of $P(t/2)/\sigma_s^2$

1204958

Since the peak observed with a period of averaging equal to the sampling period is just the average, the peak-to-mean ratio must approach unity as averaging interval increases.

It is physically obvious that the peak-to-mean ratios which are observed must be a function of position in the plume, since sites much removed from the centerline must be only intermittently exposed to a finite concentration, and thus must show larger peak-to-mean ratios for the same value of averaging interval. This is exactly what Gifford's plot indicates.

Figure 23 presents the data from the Wake and Control tests in the present series along with the lines which Gifford tentatively suggested as representative of sites near and removed from the plume centerline. It appears that the control data indicate that Gifford's near-centerline curve may underestimate the variability which is observed near the centerline. However, in view of the very few tests in the control series and their bimodal nature, no really firm statement can be made. Perhaps the most critical conclusion resulting from the data in Figure 23 is that peak-to-mean ratios in wakes are somewhat greater than those for point source plumes, and may indeed be comparable to ratios observed on the ground near an elevated release. This is true even though the source for the Wake tests was at ground level in this series.

An alternate representation is enlightening in showing more consistent behavior between the various tests in the Wake and Control series. Plotting the peak-to-mean ratios as a function of averaging interval, as shown in Figure 24, indicates that all tests have about a $t^{-1/2}$ dependence on averaging interval, similar to the consistency in

1204959

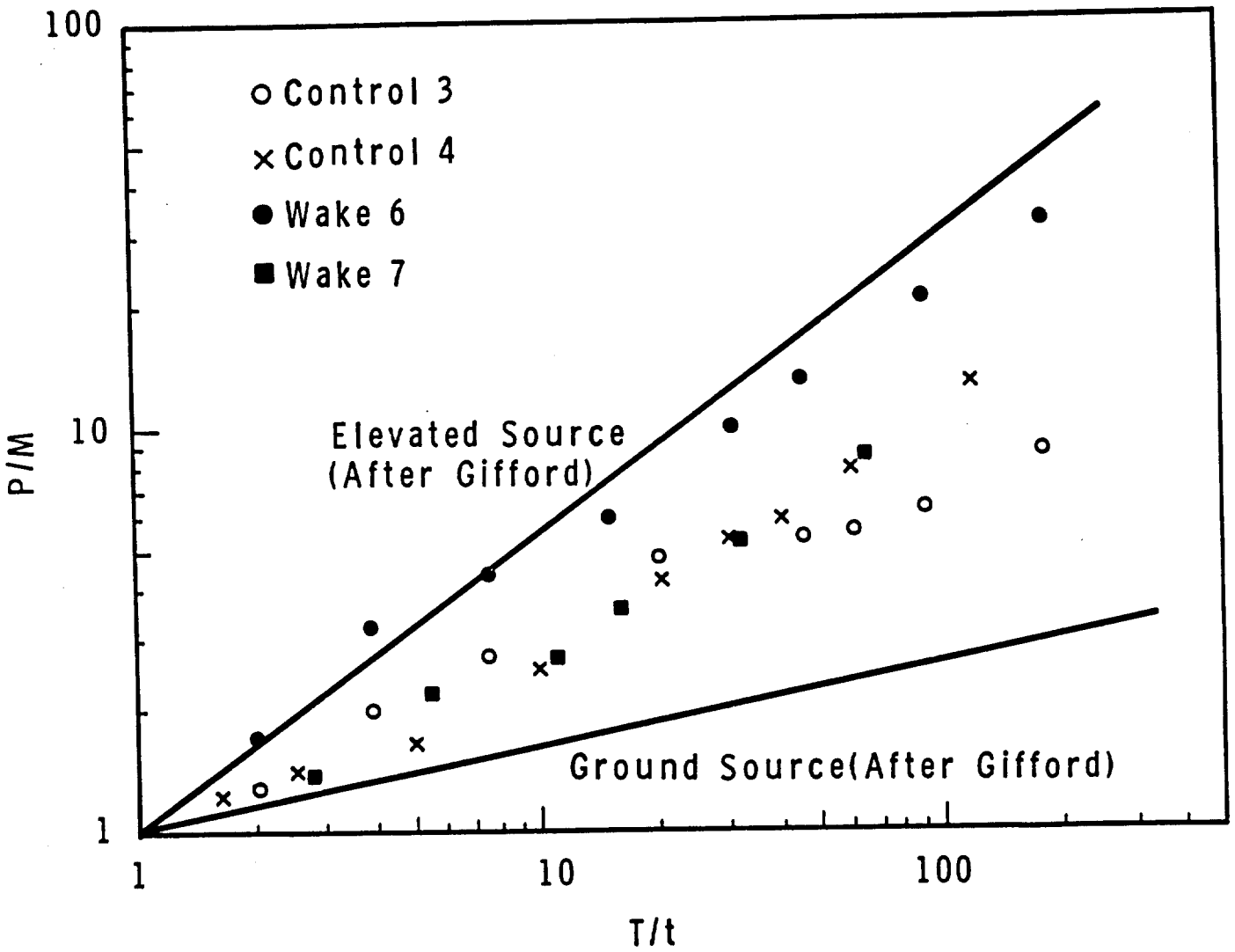

Figure 23
Peak-To-Mean Concentrations vs Proportional
Sampling Time

1204960

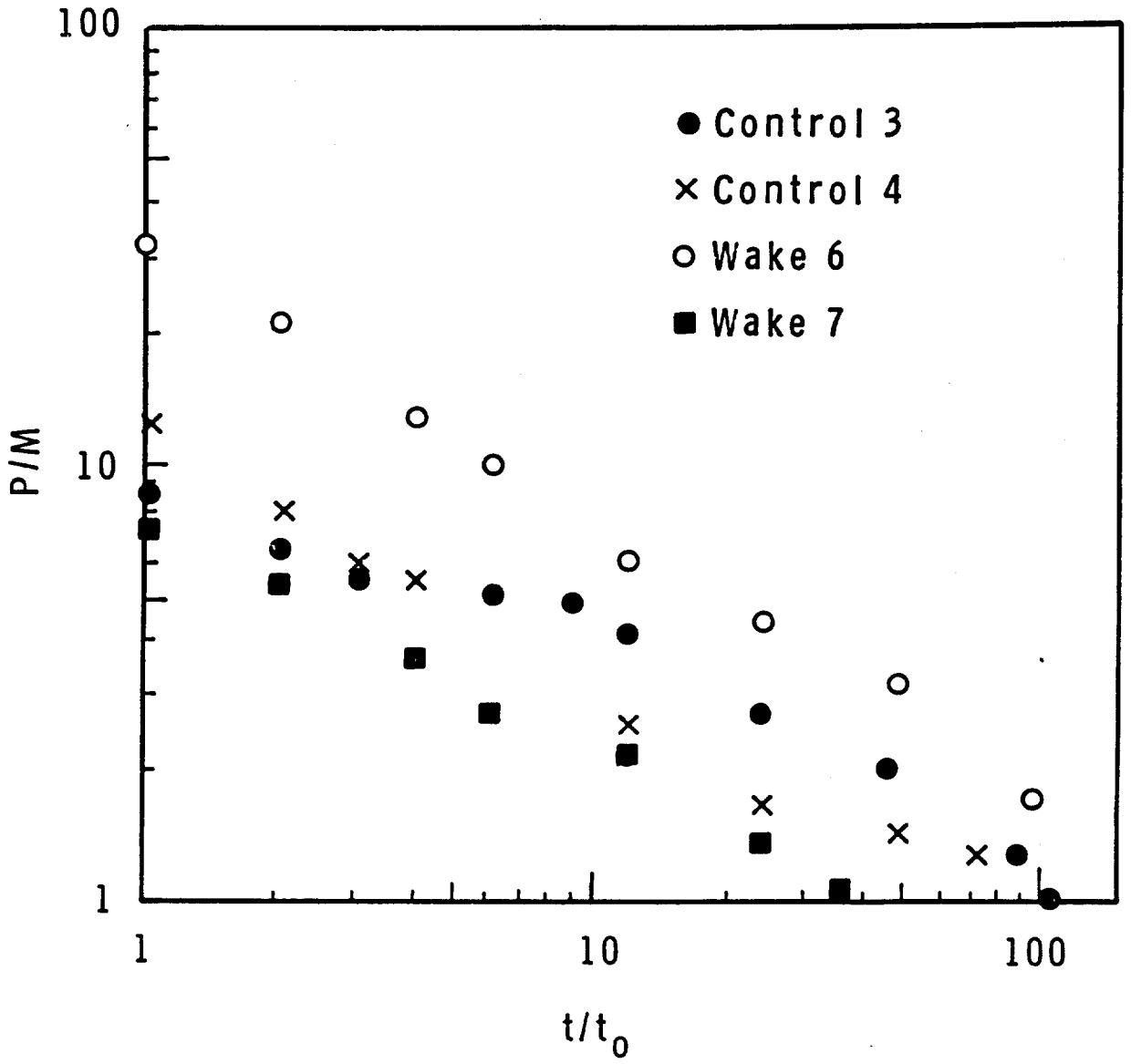

Figure 24
Peak-to-Mean Concentrations vs Sampling Interval

1204961

behavior indicated ealier in the comparison of variance for the different tests against the functional forms derived in Chapter One.

1204962

SUMMARY AND CONCLUSIONS

Contemplation of the present state of knowledge of peak-to-mean concentration ratios in atmospheric diffusion led to the consideration of the rate of change of the variance of a stationary continuous random variable with increasing smoothing. The resulting equation is

$$\frac{d\sigma_s^2}{\sigma_s^2} = 2\left[\frac{P(t/2)}{\sigma_s^2} - 1\right]\frac{dt}{t}$$

where

σ_s^2 is the variance of the smoothed variable

t is the smoothing interval

P(t/2) is the autocovariance of the unsmoothed variable at lag t/2. Since no additional assumptions were introduced concerning the nature of the variable, the equation applies to a more general class of random variables than concentration, but attention was restricted to verifying the equation for variations in concentration in this work.

A short series of four tests was carried out to gather data with which to test the theoretical results. Two tests were conducted in point source plumes and two in the cavity region in the lee of a large building. Five second averages of concentration were measured by a real-time sampler from which variances were calculated after differing periods of smoothing were applied.

The data indicated that the simple linear hypothesis that $2\left[(P(t/2)/\sigma_s^2) - 1\right] = b + kt$ produced good results for both point-source and wake concentration histories, and that calculations of the autocovariance function from

1204963

$$P(t/2) = \frac{1}{2}\left[2+b+kt\right] \sigma_s^2$$

yielded fair estimates of the observed autocovariance function. An alternate solution containing a single adjustable constant was shown to yield good results, also, but at the expense of a less tractable functional form, following from the assumption that $2\left[(P(t/2)/\sigma_s^2) - 1\right] = e^{kt}$.

A second result from the data analysis pointed to the probability that peak-to-mean concentration ratios in building wakes from ground level sources are quite comparable to those observed from elevated sources. It seems likely, then, that elevated sources discharging into or over building wakes will lead to peak-to-mean ratios which will exceed elevated source peak-to-mean ratios, due to the intermittent entrainment and release of an elevated plume in a wake. Future work should examine this possibility, since peak-to-mean ratios are of considerable interest in the diffusion of some types of toxic effluents. Future work should also continue examination of the applicability of the governing equation to other types of random variables, such as turbulent components of wind, or temperature, and seek alternate solutions which require less restrictive assumptions about the behavior of P(t/2). Some profit may result, also, from the contemplation of the unification which apparently results from using the variance as a tool, since it seems that regardless of the mechanism which produces the fluctuations of a variable, a single equation can describe the changing variance of any progressively smoothed random variable.

1204964

REFERENCES

Barad, M. L., and J. J. Fuquay, 1962: The Green Glow Diffusion Program. Geophysical Research Papers No. 73, Air Force Cambridge Research Laboratories, Bedford, Mass.

Barry, P. J., 1964: "Estimation of downwind concentration of airborne effluents discharged in the neighborhood of buildings." AECL-2043, Atomic Energy of Canada, Ltd., Chalk River, Ontario.

Birkhoff, G., and E. H. Zarantonello, 1957: Jets, Wakes, and Cavities. Academic Press, New York.

Csanady, G. T., 1967: "Concentration fluctuations in turbulent diffusion." Journal of the Atmospheric Sciences. Vol. 24, Jan., 1967, p 21-28.

Culkowski, W. M., 1967: "Estimating the effect of buildings on plumes from short stacks." Nuclear Safety. Vol. 8, No. 3, Spring, 1967, p 257-259.

Davies, P.O.A.L., and D. J. Moore, 1964: "Experiments on the behavior of effluent emitted from stacks at or near the roof level of tall reactor buildings." International Journal of Air and Water Pollution. Vol. 8, p 515-533.

Evans, B. H., 1957: "Natural airflow around buildings." Texas Engieering Experiment Station Research Report. No. 59, College Station, Texas.

1204965

Faoro, R. B., 1965: "A study of sample averaging times and peak-to-mean ratios for gaseous pollutants." Air Pollution Control Association. Preprint, 65-90.

Genikhovich, E. L., and V. P. Gracheva, 1965: "Analysis of dispersion of horizontal fluctuation of wind direction." Glavnaia Geofizicheskaia Observatoriia, Trudy. No. 172, p 42-47, Leningrad.

Gifford, F., 1959: "Statistical properties of a fluctuating plume dispersion model." Advances in Geophysics. Vol. 6, p 117-137, Academic Press, New York.

Gifford, F., 1960: "Peak to average concentration ratios according to a fluctuating plume dispersion model." International Journal of Air Pollution. Vol 3, No. 4, p 253-260.

Green, H. L., and W. R. Lane: Particulate Clouds. E and FN Spon., Ltd., London.

Halitsky, J., 1963: "Gas diffusion near buildings." Geophysical Sciences Laboratory Report. 63-3, New York University, New York.

Halitsky, J., J. Golden, P. Halpern, and P. Wu, 1963: Wind tunnel tests of gas diffusion from a leak in the shell of a nuclear power reactor." Geophysical Sciences Laboratory Report. 63-2, New York University, New York.

Halitsky, J., 1965: "Estimation of stack height required to limit contamination of building air intakes." Industrial Hygiene Journal, March-April, 1965, p 106-116.

1204966

Hinds, W. T., 1968: "The variance of an increasingly smoothed random variable." Proceedings of the U. S. Atomic Energy Commission 1967 Micrometeorological Information Symposium, Chalk River, Ontario. (Published at Chalk River, Ontario.)

Hohenleiten, H. L. von, and E. F. Wolf, 1942: "Wind tunnel tests to establish stack height for Riverside generating station." Transactions of the American Society of Mechanical Engineers. Oct., 1942, p 671-683.

Islitzer, N. F., and R. K. Dumbauld, 1963: "Atmospheric diffusion - deposition studies over flat terrain." International Journal of Air and Water Pollution, Vol. 7, p 999-1022.

Islitzer, N. F., 1965: "Aerodynamic effects of large reactor complexes upon atmospheric turbulence and diffusion." U. S. Atomic Energy Commission, IDO 12041, May, 1965.

Martin, J. E., 1965: "The correlation of wind tunnel and field measurements of gas diffusion using Krypton-85 as a tracer." University of Michigan Phoenix Project. 272, Ann Arbor.

Munn, R. E., and A.F.W. Cole, 1965: "Turbulence and diffusion in the wake of a building." Air Pollution Control Association. Preprint, 65-41.

Nickola, P. W., M. O. Rankin, M. F. Scoggins, and E. M. Sheen, 1967: "A system for recording air concentrations of zinc-sulfide fluorescent pigment on a real-time scale." Journal of Applied Meteorology. Vol. 6, April, p 430-433.

1204967

Pasquill, F., 1962: Atmospheric Diffusion. Van Nostrand, New York.

Pasquill, F., 1963: "Some comments on the design and interpretation of diffusion experiments." International Journal of Air and Water Pollution. Vol. 7, p 937-941

Sehmel, G. A., 1966: "Subisokinetic sampling of particles in an air-stream." AEC Research and Development Report, BNWL-217, Pacific Northwest Laboratory, Richland, Washington.

Sherlock, R. H., and E. A. Stalker, 1940: "The control of gases in the wake of smokestacks." Mechanical Engineering. June, 1940, p 455-458.

Simpson, C. L., 1961: "Estimates of deposition of matter from a continuous point source in a stable atmosphere." U. S. Atomic Energy Commission Report, HW-69292, Pacific Northwest Laboratory, Richland, Washington.

Singer, I. A., 1960: "The relationship between peak and mean concentrations." Journal of the Air Pollution Control Association. Vol. 11, No. 7, p 336-341.

Singer, I. A., K. Imai, and R. G. del Campo, 1963: "Peak-to-mean pollutant concentration ratios for various terrain and vegetation cover." Journal of the Air Pollution Control Association. Vol. 13, No. 1, p 40-42.

1204968

APPENDIX I

CONCENTRATIONS MEASURED BY THE SORTS

TEST C-3

Release time 15 minutes

$\bar{x} = 0.656 \times 10^{-4}$ gm/m^3

$x/\bar{x}$

.27	.388	1.31	1.67	.434	.0855
2.67	.137	.274	3.76	.64	.388
4.80	0	.055	1.84	1.88	.171
4.26	0	.055	2.01	1.71	.0855
4.80	.0855	.110	1.07	.434	.0855
4.00	.125	.055	2.05	1.26	.0434
4.00	.051	.055	.295	.0855	.0434
8.56	1.87	.0274	.342	.0434	.126
3.12	2.91	.110	.81	.0434	.296
5.85	4.43	.605	1.84	1.59	.126
4.64	3.17	.548	.251	4.01	.171
1.68	1.28	.274	.126	2.49	.855
.32	2.25	.137	.0855	5.05	.855
0	5.23	.137	.216	4.62	.855
0	1.01	.685	.126	1.59	.855
.163	.342	.548	1.67	2.01	.434
2.52	.228	.274	2.78	.342	.855
1.48	.171	.274	3.68	.903	0
2.56	.194	.410	2.96	2.86	0
2.96	.080	1.37	2.05	.434	0
2.28	.0548	1.78	.685	.171	
2.14	.274	.685	.251	.171	
2.38	.410	.137	2.171	.0855	
.605	.194	1.78	.0855	.126	
.11	.110	3.44	.251	.126	
.082	0	.821	.775	.56	
.055	.410	.274	1.93	1.03	
.082	0	.137	.434	.434	
.082	1.15	0	.171	1.12	
.820	.331	.125	.560	.514	
.685	.274	.935	.251	.217	
3.48	.490	1.20	.171	.0855	

1204969

TEST C-4

Release time 10 minutes

$\bar{x} = 0.310 \times 10^{-4}$ gm/m^3

$x/\bar{x}$			
.58	0	.182	.182
0	0	.182	.092
0	0	0	.092
0	0	.092	.092
0	0	0	.182
.87	.181	.182	.092
5.80	0	1.19	.092
3.49	0	4.83	0
1.16	0	1.72	0
4.07	0	3.73	0
2.91	0	7.07	0
2.62	0	2.08	0
.58	.46	.92	3.10
0	2.28	.73	12.3
0	4.45	.267	2.37
0	1.81	.267	1.26
1.74	6.0	.363	.533
2.52	9.55	5.45	.363
0	1.98	1.65	.363
.58	.73	.46	.363
.87	1.19	1.65	.915
0	.533	.63	0
0	.363	1.09	0
0	.182	.46	0
0	.182	.363	0
0	.092	1.55	0
0	.092	1.57	0
0	.092	.63	0
0	.092		0
0	0		0
0	0		0

1204970

TEST W-6

Release tune 15 minutes

$\bar{x} = 4.83 \times 10^{-4}$ gm/m^3

$x/\bar{x}$

.238	.156	.010	.064	2.31	4.33
.431	.183	.046	.010	1.12	2.30
.476	.532	.092	.027	2.98	1.76
.770	.623	.027	.083	2.67	1.23
.219	.414	.018	.120	1.20	1.23
.257	.165	.018	.073	4.14	1.06
.165	.073	.027	.046	1.64	
.238	.120	.329	.046	3.70	
.092	.209	.055	.100	3.70	
.055	.147	.055	.173	.530	
.073	.476	0	.110	.800	
.055	.230	0	.064	6.44	
.046	.046	0	.120	8.11	
.128	.128	0	.037	3.35	
.046	.128	0	0	.965	
.064	.100	.110	0	1.32	
.046	.120	.193	0	2.92	
.120	.110	.248	.083	3.98	
.092	.120	.267	.128	10.41	
.238	.202	.642	.110	6.09	
.696	.156	.055	.092	1.23	
1.37	.083	.120	.055	1.06	
.348	.037	0	.120	1.15	
.257	.037	.092	.385	1.32	
.248	.071	.046	.642	.706	
.092	.092	.018	.487	2.38	
.073	0	.018	.100	3.98	
.311	.412	0	.083	.530	
.183	.173	.027	.209	4.41	
.942	.173	.018	.092	6.79	
.302	.018	.055	.010	2.92	
.193	0	.348	0	2.30	
.230	.018	.202	.027	22.36	
.677	.284	.010	.037	20.91	
.202	.083	.055	1.50	6.17	

1204971

TEST W-7

Release time 6 minutes

$\bar{\chi} = 0.817 \times 10^{-4}$ gm/m^3

$\chi/\bar{\chi}$	
.052	.522
.261	.365
7.47	.680
3.29	.680
2.14	.732
1.51	2.03
1.10	1.15
.887	.680
1.73	.261
2.46	.261
2.09	.313
2.03	.418
1.36	.836
.836	1.21
.365	.574
.261	.784
.473	1.04
.261	.888
.626	.941
.418	.993
.626	.836
.313	1.04
.365	.888
.365	.313
.574	.313
.680	.313
1.21	.626
1.51	.680
1.10	.522
1.25	.888
1.83	0
.574	0
.261	0
.365	0
.313	0

1204972